SIGGRAPH THINK BEYOND

2020 S2020.SIGGRAPH.ORG

PATH-SPACE DIFFERENTIABLE RENDERING

Cheng Zhang[1], Bailey Miller[2], Kai Yan[1], Ioannis Gkioulekas[2], Shuang Zhao[1]

[1]University of California, Irvine
[2]Carnegie Mellon University

WHY WE NEED DIFF. RENDERING?

- Inverse rendering
  - Enabling gradient-based optimization

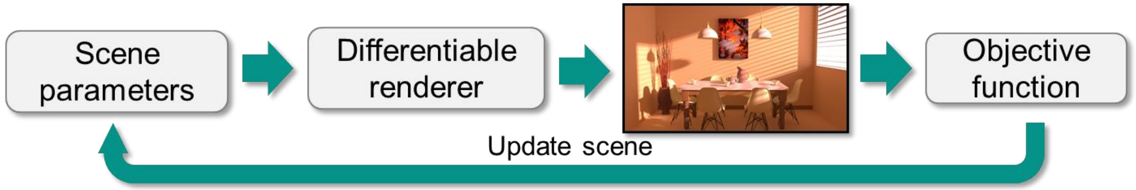

- Machine learning
  - Backpropagation through rendering

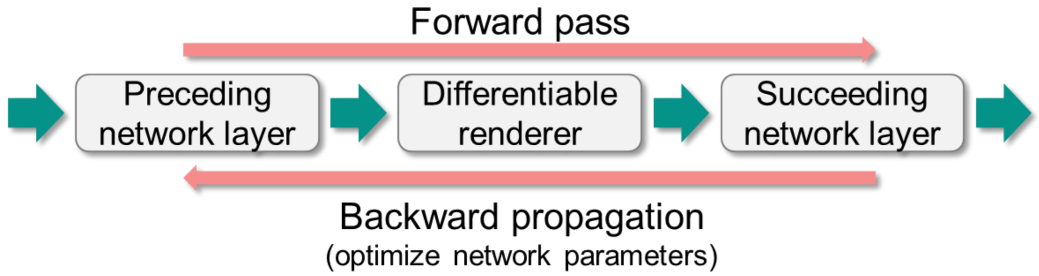

CHALLENGES

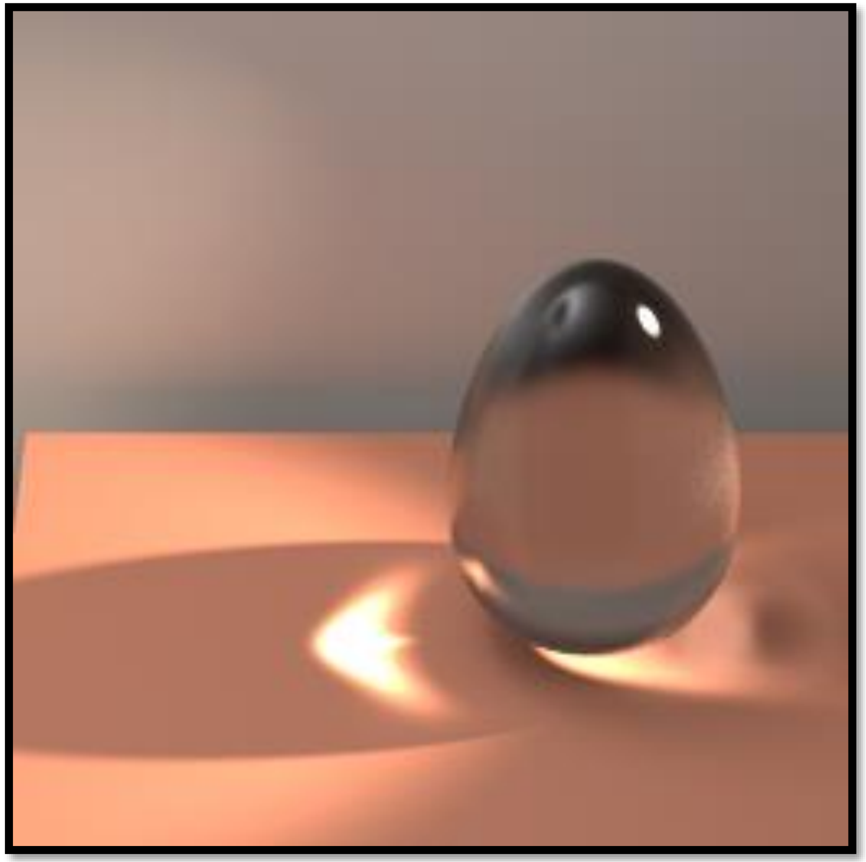

Complex light transport effects

Complex geometry

Li et al. 2018 Zhang et al. 2019 Loubet et al. 2019

Our method addresses both challenges efficiently!

- Handling complex geometry
  - [Li et al. 2018, Zhang et al. 2019] Expensive silhouette detection
  - [Loubet et al. 2019] Biased approximation
- Handling complex light transport effects
  - All previous methods Unidirectional path tracing only

PREVIEW OF OUR RESULTS

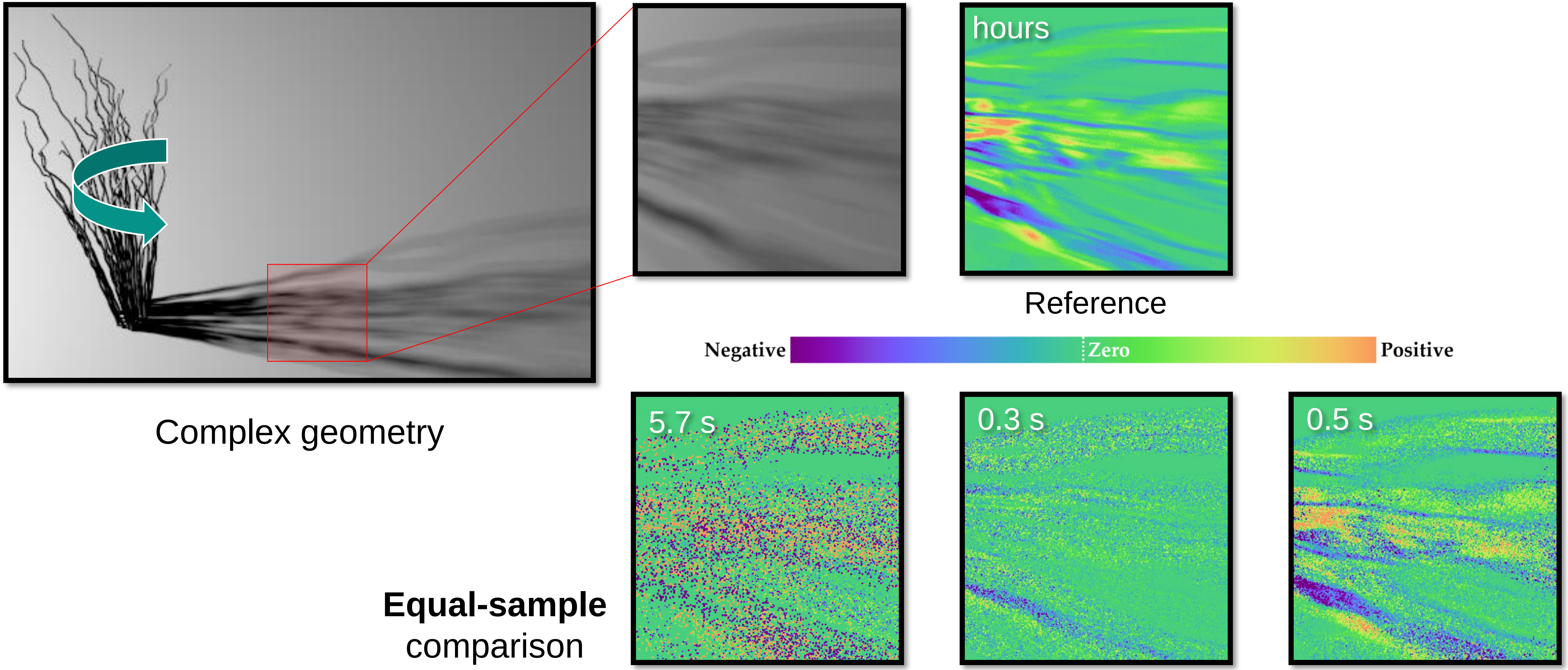

Complex geometry

Reference

Equal-sample comparison

[Zhang et al. 2019]

[Loubet et al. 2019]

Ours

PREVIEW OF OUR RESULTS

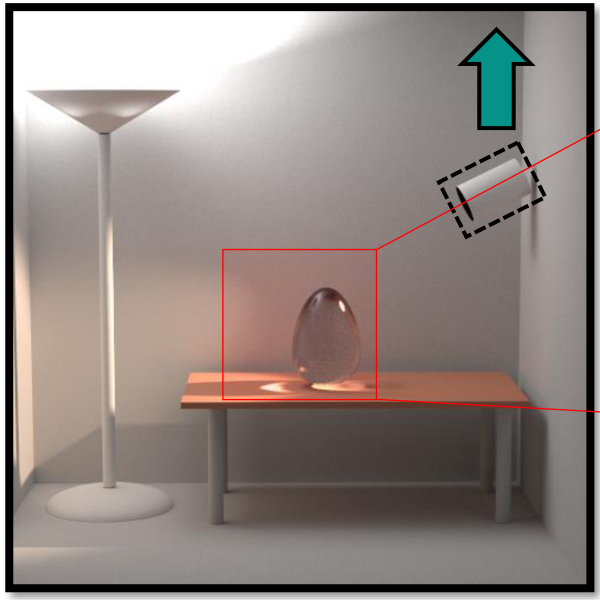

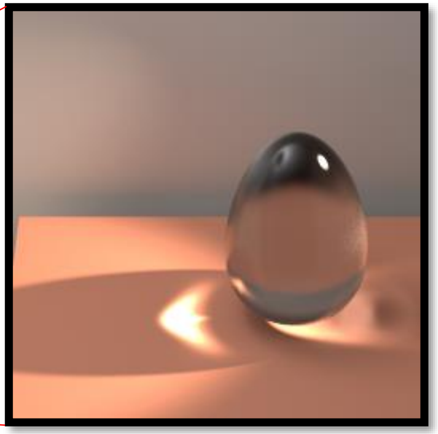

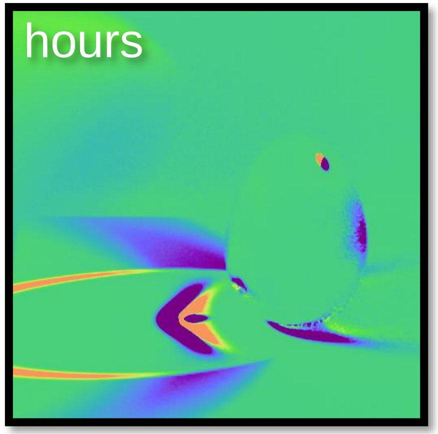

Reference

Negative

Positive

Complex light transport effects

Equal-sample
comparison

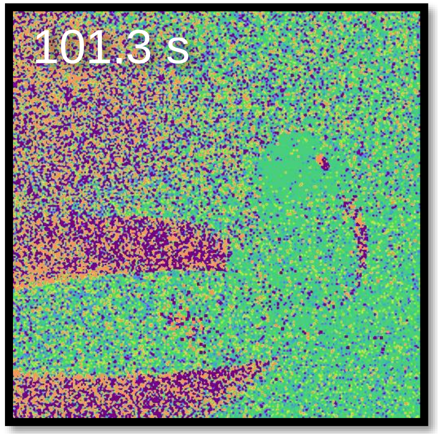

[Zhang et al. 2019]

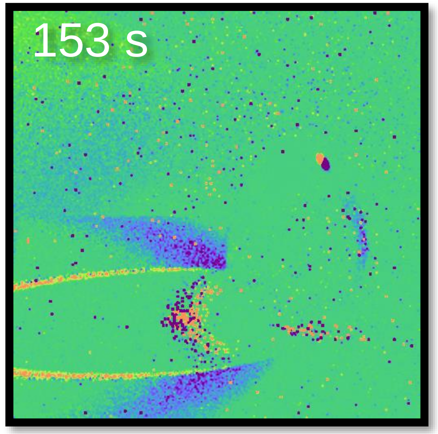

[Loubet et al. 2019]

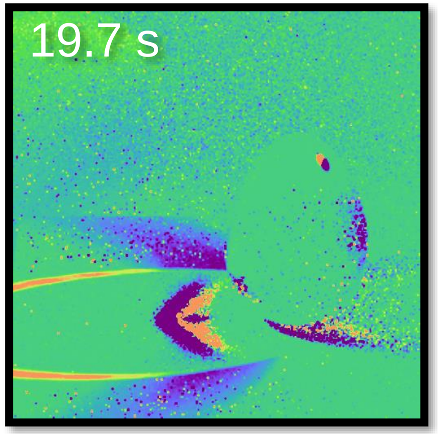

Ours

PRELIMINARIES

REYNOLDS TRANSPORT THEOREM

$$\frac{\mathrm{d}}{\mathrm{d}\pi}\int_{\Omega} f\,\mathrm{d}A \overset{?}{=} \int_{\Omega} \frac{\mathrm{d}f}{\mathrm{d}\pi}\,\mathrm{d}A + \int_{\partial\Omega} g\,\mathrm{d}l$$

Reynolds transport theorem
Generalization of Leibniz's rule

Interior integral

Boundary domain

boundary integral

||

discontinuity points ∪ boundary of domain Ω

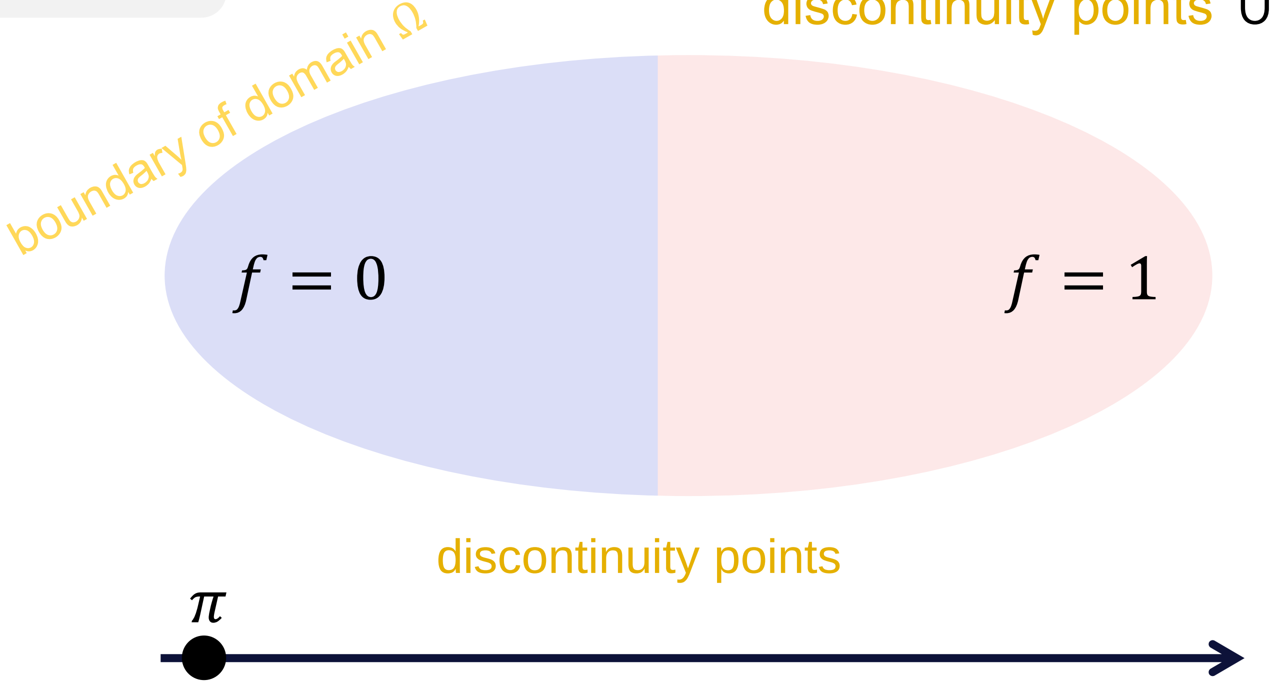

REYNOLDS TRANSPORT THEOREM

π: size of the emitter

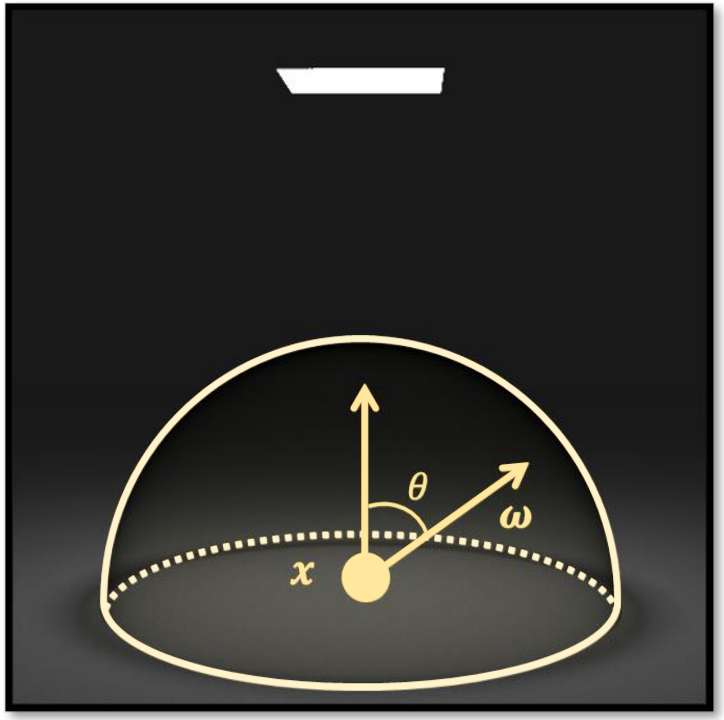

Irradiance at $\boldsymbol{x}$

$$E = \int_{\mathbb{H}^2} L_i(\boldsymbol{\omega}) \cos\theta \, \mathrm{d}\sigma(\boldsymbol{\omega})$$

Unit hemisphere

Differential irradiance at $\boldsymbol{x}$

$$\frac{\mathrm{d}E}{\mathrm{d}\pi} = \frac{\mathrm{d}}{\mathrm{d}\pi} \int_{\mathbb{H}^2} L_i(\boldsymbol{\omega}) \cos\theta \, \mathrm{d}\sigma(\boldsymbol{\omega})$$

REYNOLDS TRANSPORT THEOREM

π: size of the emitter

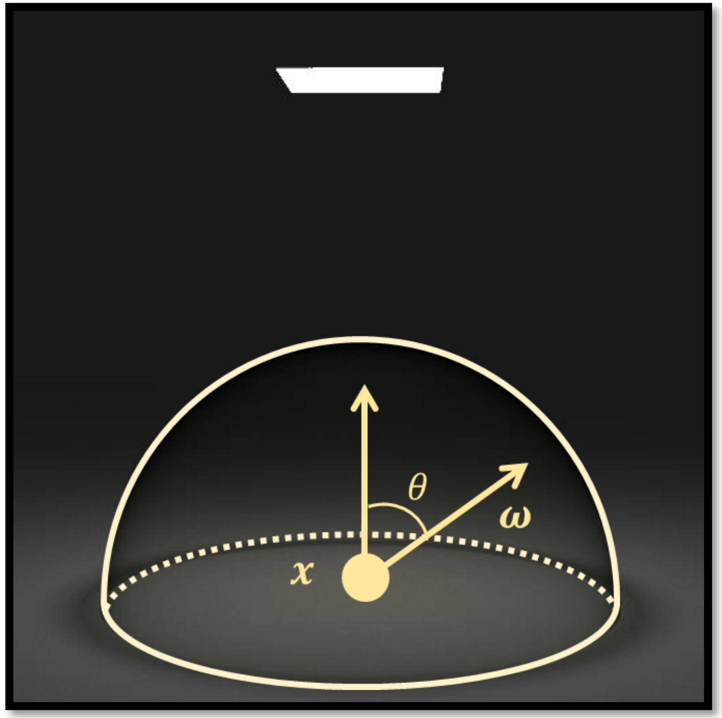

$$E = \int_{\mathbb{H}^2} L_i(\boldsymbol{\omega}) \cos\theta \, \mathrm{d}\sigma(\boldsymbol{\omega})$$

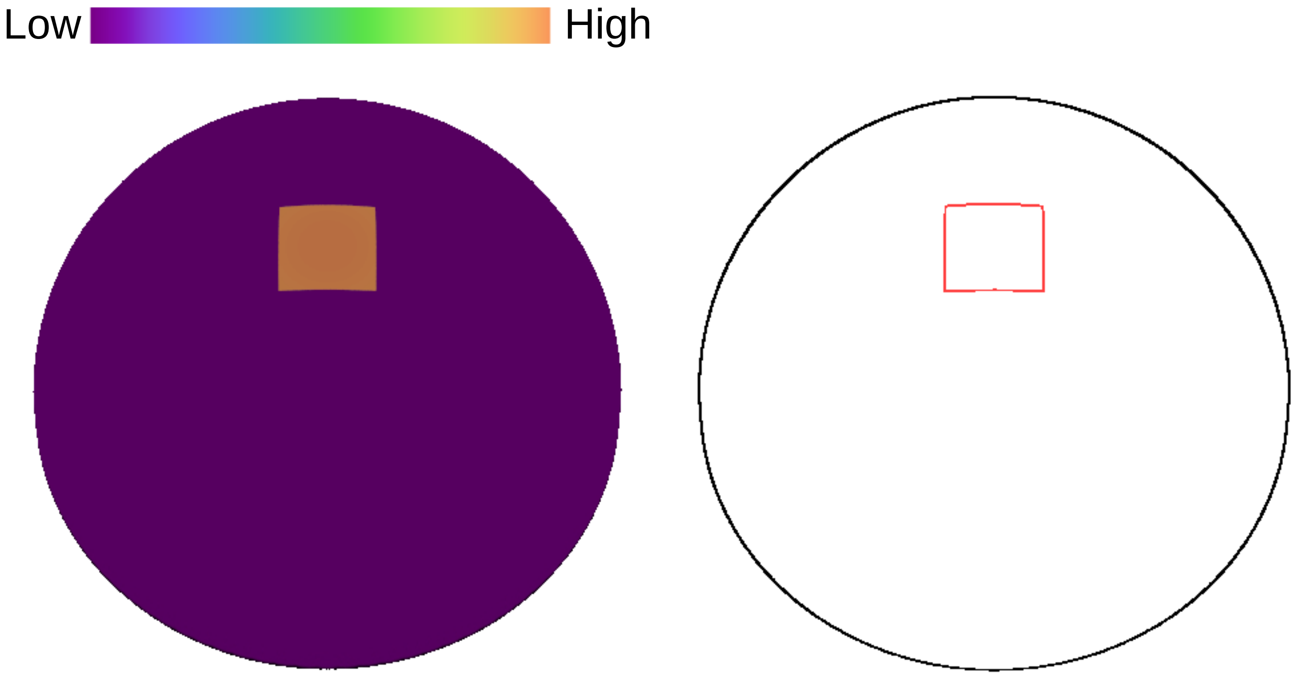

The integrand

Discontinuous points
(π-dependent)

REYNOLDS TRANSPORT THEOREM

$$E = \int_{\mathbb{H}^2} \overbrace{L_i(\boldsymbol{\omega}) \cos\theta \, \mathrm{d}\sigma(\boldsymbol{\omega})}^{f}$$

$$\frac{\mathrm{d}E}{\mathrm{d}\pi} = \int_{\mathbb{H}^2} \frac{\mathrm{d}f}{\mathrm{d}\pi} \mathrm{d}\sigma + \int_{\partial\mathbb{H}^2} g \, \mathrm{d}l$$

$= 0$ $\neq 0$

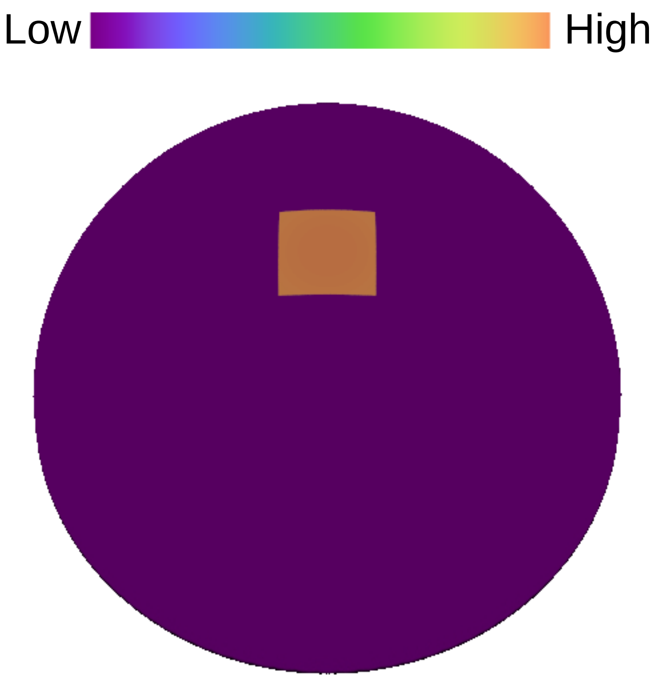

The integrand

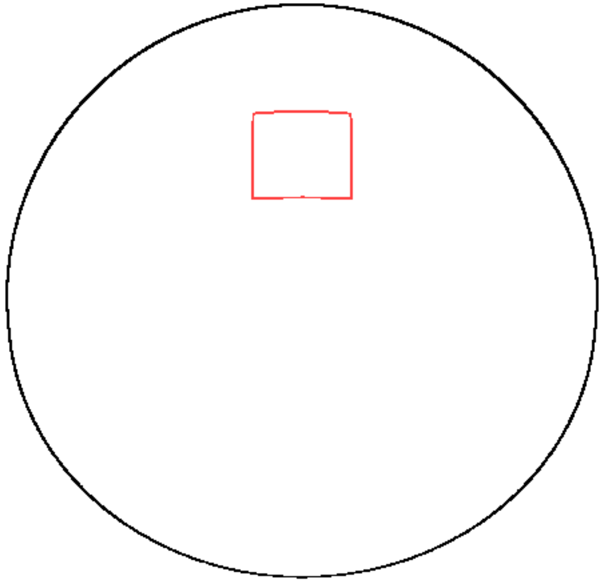

Discontinuous points
(π-dependent)

SOURCE OF DISCONTINUITIES

Boundary edge 

Sharp edge 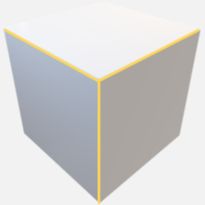

Silhouette edge 

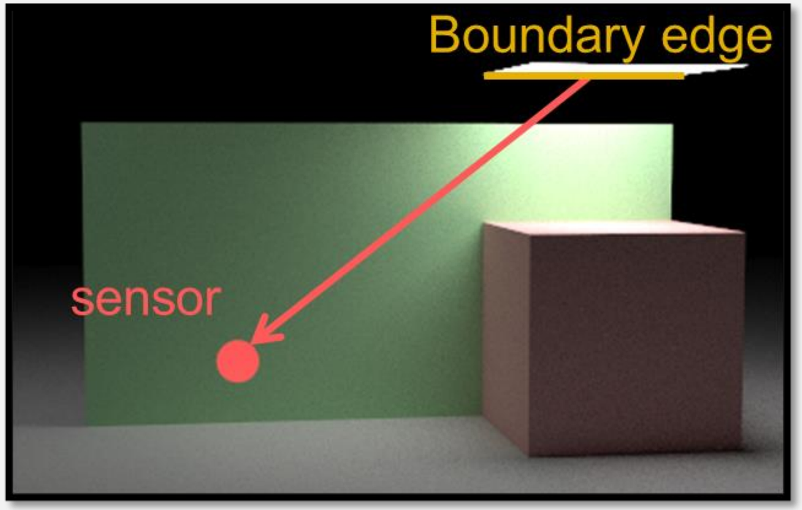

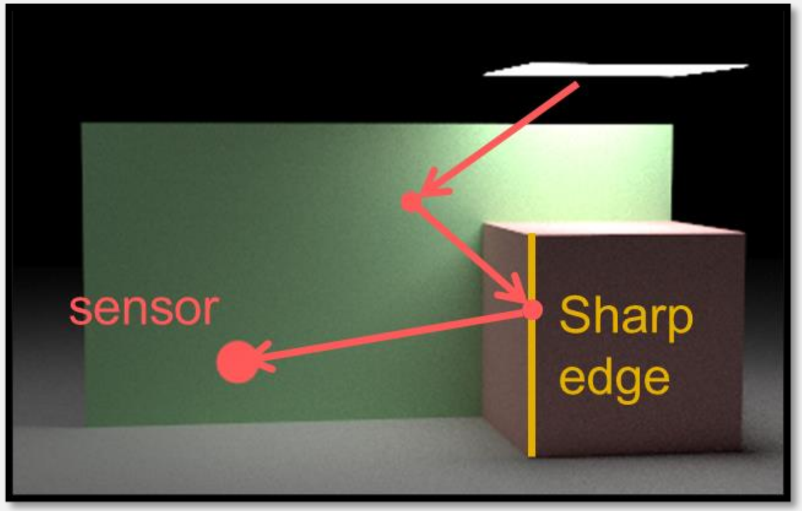

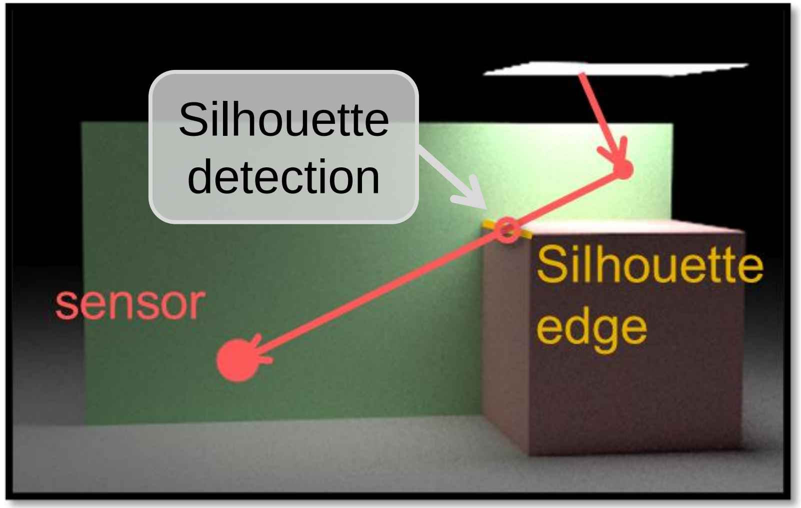

Topology-driven

Visibility-driven

OUR TECHNIQUE

OUR CONTRIBUTIONS

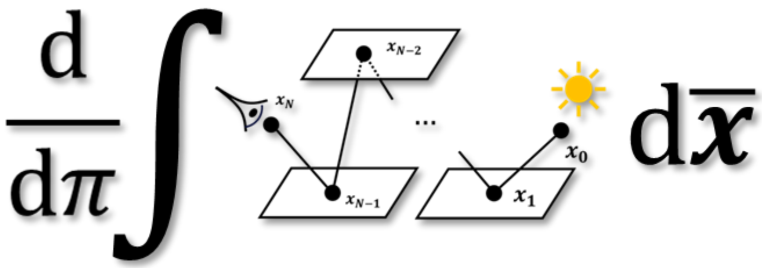

$$f(\boldsymbol{x})$$

$$\boldsymbol{x} = \mathrm{X}(\boldsymbol{p})$$

$$f(\mathrm{X}(\boldsymbol{p}))$$

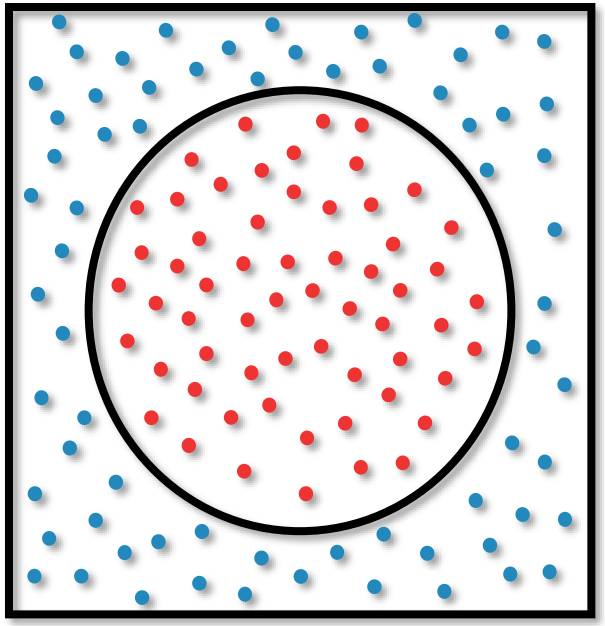

Differential path integral

Reparameterization

Monte Carlo Estimator

FORWARD PATH INTEGRAL

$$I = \int_{\Omega} f(\bar{x}) \, \mathrm{d}\mu(\bar{x})$$

Measurement contribution function

Path space

Area-product measure

- Introduced by Veach [1997]
- Foundation of sophisticated Monte Carlo algorithms (e.g., BDPT, MCMC rendering)

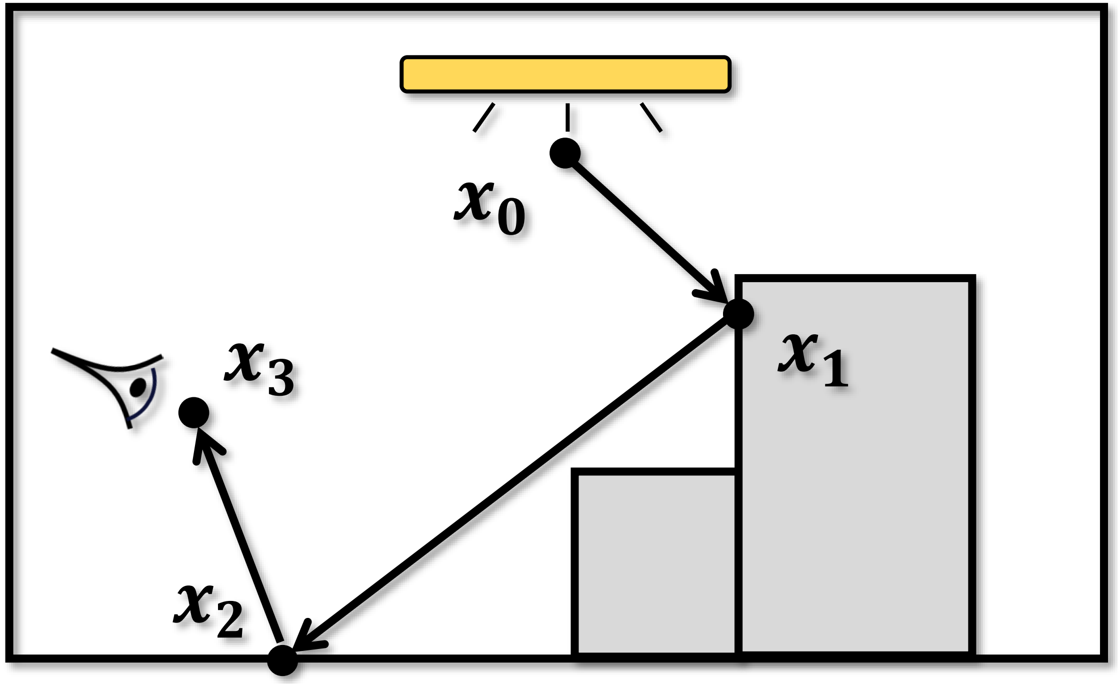

Light path $\bar{x} = (x_0, x_1, x_2, x_3)$

DIFFERENTIAL PATH INTEGRAL

Path Integral

A generalization of Reynolds theorem

$$I = \int_{\Omega} f(\bar{\boldsymbol{x}})\,\mathrm{d}\mu(\bar{\boldsymbol{x}}) \quad \Rightarrow \quad \frac{\mathrm{d}I}{\mathrm{d}\pi} = \;?$$

We now derive $\partial I_N/\partial\pi$ in Eq. (25) using the recursive relations provided by Eqs. (21) and (24). Let

$$h_n^{(0)} := \left[\prod_{n'=n+1}^{N} g(\boldsymbol{x}_{n'};\boldsymbol{x}_{n'-2},\boldsymbol{x}_{n'-1})\right] W_e(\boldsymbol{x}_N \to \boldsymbol{x}_{N-1}), \tag{52}$$

$$h_n^{(1)} := \sum_{n'=n+1}^{N} \kappa(\boldsymbol{x}_{n'})\,V(\boldsymbol{x}_{n'}), \tag{53}$$

$$\Delta h_{n,n'}^{(0)} := h_n^{(0)}\,\Delta g(\boldsymbol{x}_{n'};\boldsymbol{x}_{n'-2},\boldsymbol{x}_{n'-1})/g(\boldsymbol{x}_{n'};\boldsymbol{x}_{n'-2},\boldsymbol{x}_{n'-1}), \tag{54}$$

for $0 \le n < n' \le N$. We omit the dependencies of $h_n^{(0)}$, $h_n^{(1)}$, and $\Delta h_{n,n'}^{(0)}$ on $\boldsymbol{x}_{n+1},\ldots,\boldsymbol{x}_N$ for notational convenience.

We now show that, for all $0 \le n < N$, it holds that

$$h_n(\boldsymbol{x}_n;\boldsymbol{x}_{n-1}) = \int_{\mathcal{M}^{N-n}} h_n^{(0)} \prod_{n'=n+1}^{N} \mathrm{d}A(\boldsymbol{x}_{n'}), \tag{55}$$

and

$$\dot{h}_n(\boldsymbol{x}_n;\boldsymbol{x}_{n-1}) = \int_{\mathcal{M}^{N-n}} \left[\left(h_n^{(0)}\right)^{\cdot} - h_n^{(0)} h_n^{(1)}\right] \prod_{n'=n+1}^{N} \mathrm{d}A(\boldsymbol{x}_{n'}) + \sum_{n'=n+1}^{N} \int \Delta h_{n,n'}^{(0)}\, V_{\overline{\partial\mathcal{M}}_{n'}}(\boldsymbol{x}_{n'})\,\mathrm{d}\ell(\boldsymbol{x}_{n'}) \prod_{\substack{n<i\le N\\ i\ne n'}} \mathrm{d}A(\boldsymbol{x}_i), \tag{56}$$

where the integral domain of the second term on the right-hand side, which is omitted for notational clarity, is $\mathcal{M}(\pi)$ for each $\boldsymbol{x}_i$ with $i \ne n'$ and $\overline{\partial\mathcal{M}}_{n'}(\pi)$, which depends on $\boldsymbol{x}_{n'-1}$, for $\boldsymbol{x}_{n'}$.

It is easy to verify that Eqs. (55) and (56) hold for $n = N-1$. We now show that, if they hold for some $0 < n < N$, then it is also the case for $n-1$. Let $g_{n-1} := g(\boldsymbol{x}_n;\boldsymbol{x}_{n-2},\boldsymbol{x}_{n-1})$ for all $0 < n \le N$. Then,

$$\begin{aligned} h_{n-1}(\boldsymbol{x}_{n-1};\boldsymbol{x}_{n-2}) &= \int_{\mathcal{M}} g_{n-1} \int_{\mathcal{M}^{N-n}} h_n^{(0)} \prod_{n'=n+1}^{N} \mathrm{d}A(\boldsymbol{x}_{n'})\,\mathrm{d}A(\boldsymbol{x}_n) \\ &= \int_{\mathcal{M}^{N-n+1}} h_{n-1}^{(0)} \prod_{n'=n}^{N} \mathrm{d}A(\boldsymbol{x}_{n'}), \end{aligned} \tag{57}$$

and

$$\begin{aligned} &\dot{h}_{n-1}(\boldsymbol{x}_{n-1};\boldsymbol{x}_{n-2}) \\ &= \int_{\mathcal{M}} \left[\dot{g}_{n-1} h_n + g_{n-1}(\dot{h}_n - h_n\,\kappa(\boldsymbol{x}_n)\,V(\boldsymbol{x}_n))\right] \mathrm{d}A(\boldsymbol{x}_n) \\ &\quad + \int_{\overline{\partial\mathcal{M}}_n} \Delta g_{n-1}\, h_n\, V_{\overline{\partial\mathcal{M}}_n}\,\mathrm{d}\ell(\boldsymbol{x}_n) \\ &= \int_{\mathcal{M}^{N-n+1}} \left\{\dot{g}_{n-1} h_n^{(0)} + g_{n-1}\left[\left(h_n^{(0)}\right)^{\cdot} - h_n^{(0)} h_{n-1}^{(1)}\right]\right\} \prod_{n'=k}^{N} \mathrm{d}A(\boldsymbol{x}_{n'}) \\ &\quad + \sum_{n'=n+1}^{N} \int g_{n-1}\,\Delta h_{n,n'}^{(0)}\, V_{\overline{\partial\mathcal{M}}_{n'}}(\boldsymbol{x}_{n'})\,\mathrm{d}\ell(\boldsymbol{x}_{n'}) \prod_{\substack{n\le i\le N\\ i\ne n'}} \mathrm{d}A(\boldsymbol{x}_i) \\ &\quad + \int \Delta g_{n-1}\, h_n^{(0)}\, V_{\overline{\partial\mathcal{M}}_n}\,\mathrm{d}\ell(\boldsymbol{x}_n) \prod_{n'=n+1}^{N} \mathrm{d}A(\boldsymbol{x}_{n'}) \\ &= \int_{\mathcal{M}^{N-n+1}} \left[\left(h_{n-1}^{(0)}\right)^{\cdot} - h_{n-1}^{(0)} h_{n-1}^{(1)}\right] \prod_{n'=n}^{N} \mathrm{d}A(\boldsymbol{x}_{n'}) \\ &\quad + \sum_{n'=n}^{N} \int \Delta h_{n-1,n'}^{(0)}\, V_{\overline{\partial\mathcal{M}}_{n'}}(\boldsymbol{x}_{n'})\,\mathrm{d}\ell(\boldsymbol{x}_{n'}) \prod_{\substack{n\le i\le N\\ i\ne n'}} \mathrm{d}A(\boldsymbol{x}_i). \end{aligned} \tag{58}$$

Thus, using mathematical induction, we know that Eqs. (55) and (56) hold for all $0 \le n < N$.

Notice that $h_0^{(0)} = f$ and $\Delta h_{0,n'}^{(0)} = \Delta f_{n'}$, where $\Delta f_{n'}$ follows the definition in Eq. (28). Letting $n = 0$ in Eq. (56) yields

$$\dot{h}_0(\boldsymbol{x}_0) = \int_{\mathcal{M}^N} \left[\dot{f}(\bar{\boldsymbol{x}}) - f(\bar{\boldsymbol{x}}) \sum_{n'=1}^{N} \kappa(\boldsymbol{x}_{n'})\,V(\boldsymbol{x}_{n'})\right] \prod_{n'=1}^{N} \mathrm{d}A(\boldsymbol{x}_{n'}) + \sum_{n'=1}^{N} \int \Delta f_{n'}(\bar{\boldsymbol{x}})\, V_{\overline{\partial\mathcal{M}}_{n'}}\,\mathrm{d}\ell(\boldsymbol{x}_{n'}) \prod_{\substack{0<i\le N\\ i\ne n'}} \mathrm{d}A(\boldsymbol{x}_i). \tag{59}$$

Lastly, based on the assumption that h_0 is continuous in $\boldsymbol{x}_0$, Eq. (25) can be obtained by differentiating Eq. (23):

$$\begin{aligned} \frac{\partial I_N}{\partial\pi} &= \frac{\partial}{\partial\pi} \int_{\mathcal{M}} h_0(\boldsymbol{x}_0)\,\mathrm{d}A(\boldsymbol{x}_0) \\ &= \int_{\mathcal{M}} \left[\dot{h}_0(\boldsymbol{x}_0) - h_0(\boldsymbol{x}_0)\,\kappa(\boldsymbol{x}_0)\,V(\boldsymbol{x}_0)\right] \mathrm{d}A(\boldsymbol{x}_0) \\ &\quad + \int_{\overline{\partial\mathcal{M}}_0} h_0(\boldsymbol{x}_0)\, V_{\overline{\partial\mathcal{M}}_0}(\boldsymbol{x}_0)\,\mathrm{d}\ell(\boldsymbol{x}_0) \\ &= \int_{\Omega_N} \left[\dot{f}(\bar{\boldsymbol{x}}) - f(\bar{\boldsymbol{x}}) \sum_{K=0}^{N} \kappa(\boldsymbol{x}_K)\,V(\boldsymbol{x}_K)\right] \mathrm{d}\mu(\bar{\boldsymbol{x}}) \\ &\quad + \sum_{K=0}^{N} \int_{\Omega_{N,K}} \Delta f_K(\bar{\boldsymbol{x}})\, V_{\overline{\partial\mathcal{M}}_K}\,\mathrm{d}\mu'_{N,K}(\bar{\boldsymbol{x}}). \end{aligned} \tag{60}$$

Full derivation in the paper

DIFFERENTIAL PATH INTEGRAL

Path Integral

A generalization of Reynolds theorem

Differential Path Integral

$$I = \int_{\Omega} f(\bar{\boldsymbol{x}})\,\mathrm{d}\mu(\bar{\boldsymbol{x}}) \quad \Rightarrow \quad \frac{\mathrm{d}I}{\mathrm{d}\pi} = \int_{\Omega} \frac{\mathrm{d}}{\mathrm{d}\pi} f(\bar{\boldsymbol{x}})\,\mathrm{d}\mu(\bar{\boldsymbol{x}}) + \int_{\partial\Omega} g(\bar{\boldsymbol{x}})\,\mathrm{d}\mu'(\bar{\boldsymbol{x}})$$

path space ↗

Interior integral

boundary path space ↗

Boundary integral

Types of discontinuity edge:

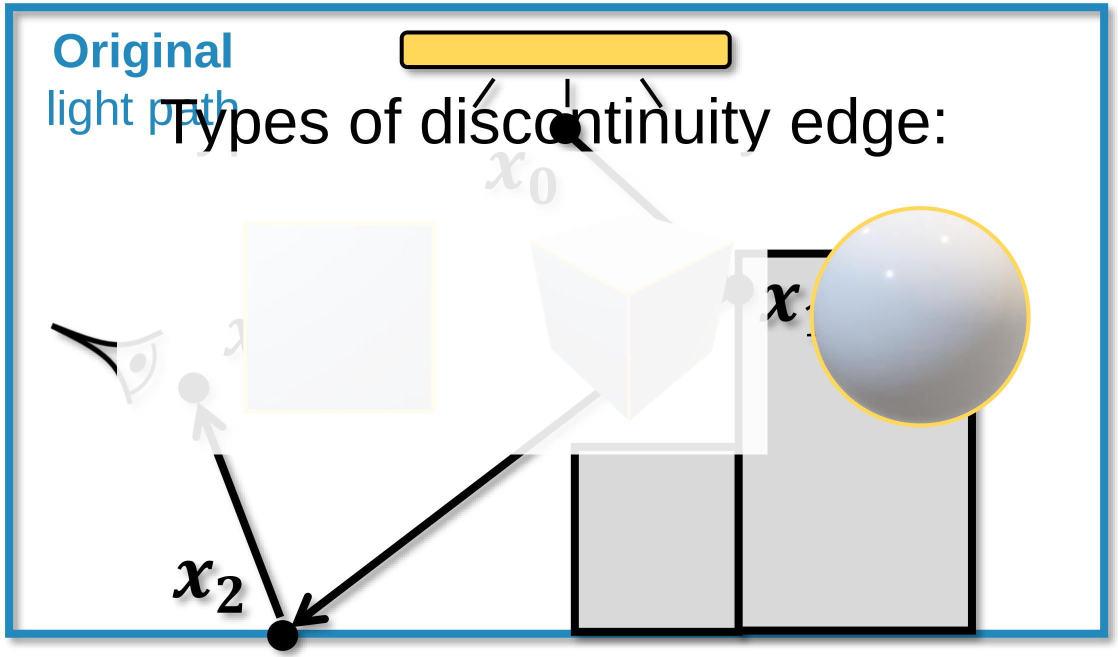

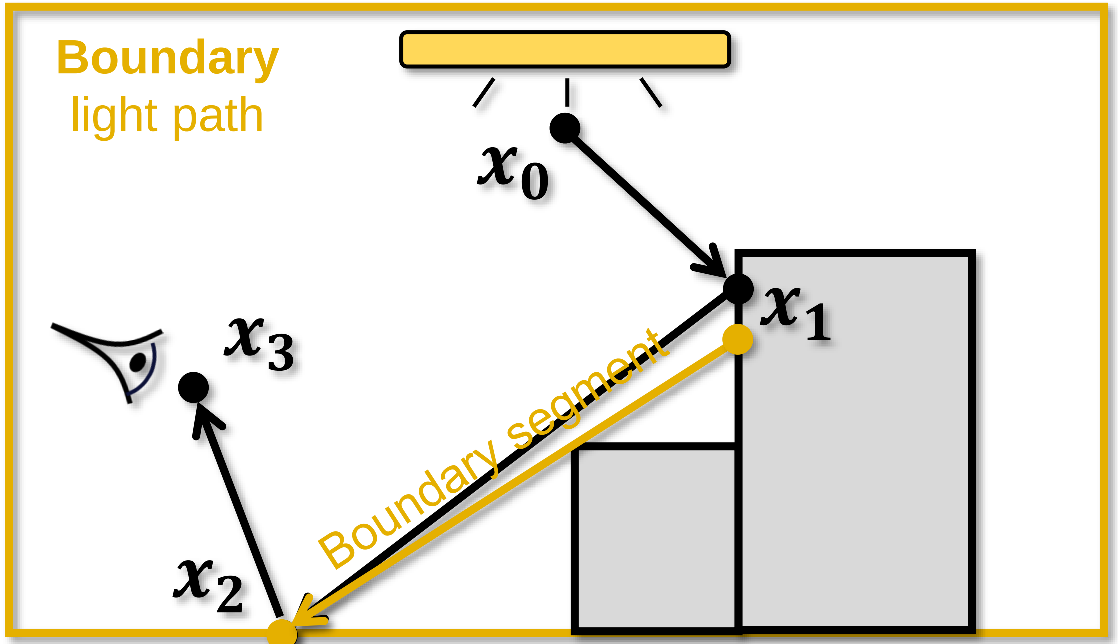

REVISIT - DIFFERENTIAL IRRADIANCE

π: size of the emitter

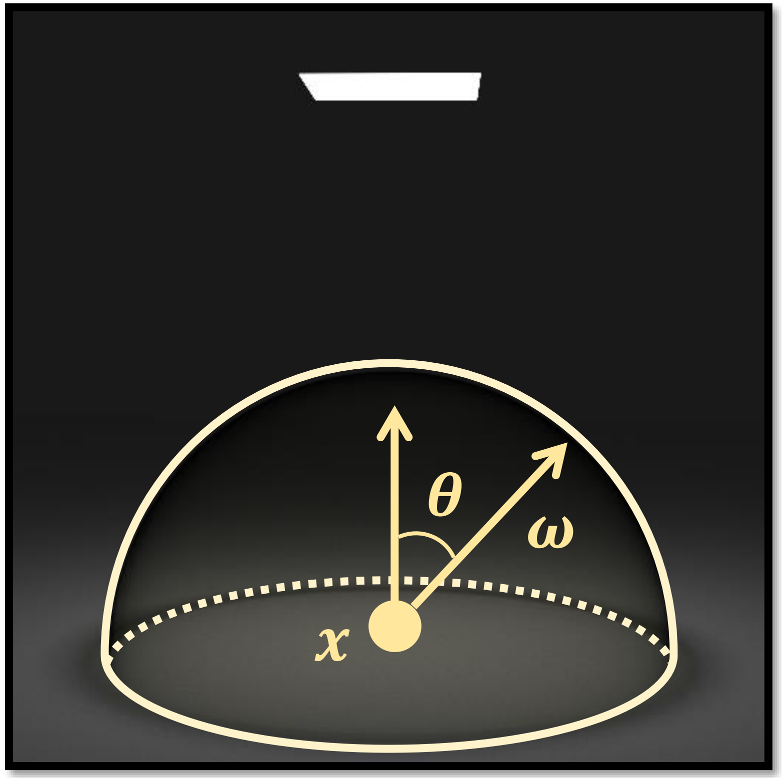

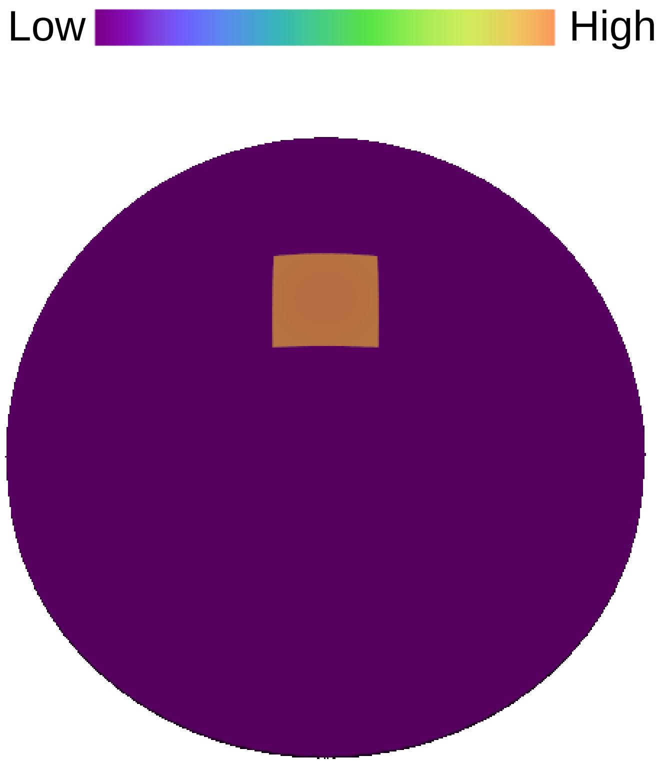

Discontinuities of f

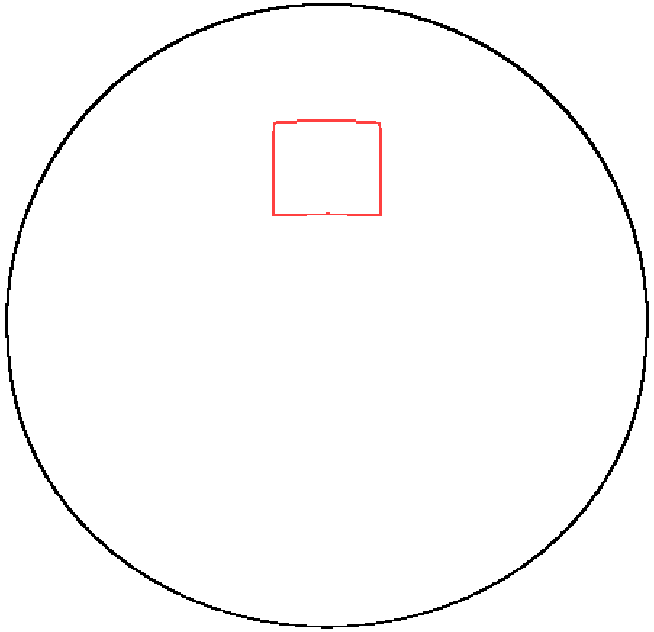

$$E = \int_{\mathbb{H}^2} \underbrace{L_i(\boldsymbol{\omega}) \cos\theta}_{f} \, \mathrm{d}\sigma(\boldsymbol{\omega})$$

Differentiation

$$\frac{\mathrm{d}E}{\mathrm{d}\pi} = \int_{\mathbb{H}^2} \frac{\mathrm{d}f}{\mathrm{d}\pi} \mathrm{d}\sigma + \int_{\partial\mathbb{H}^2} g \, \mathrm{d}l$$

$= 0$ $\neq 0$

DIFFERENTIAL IRRADIANCE

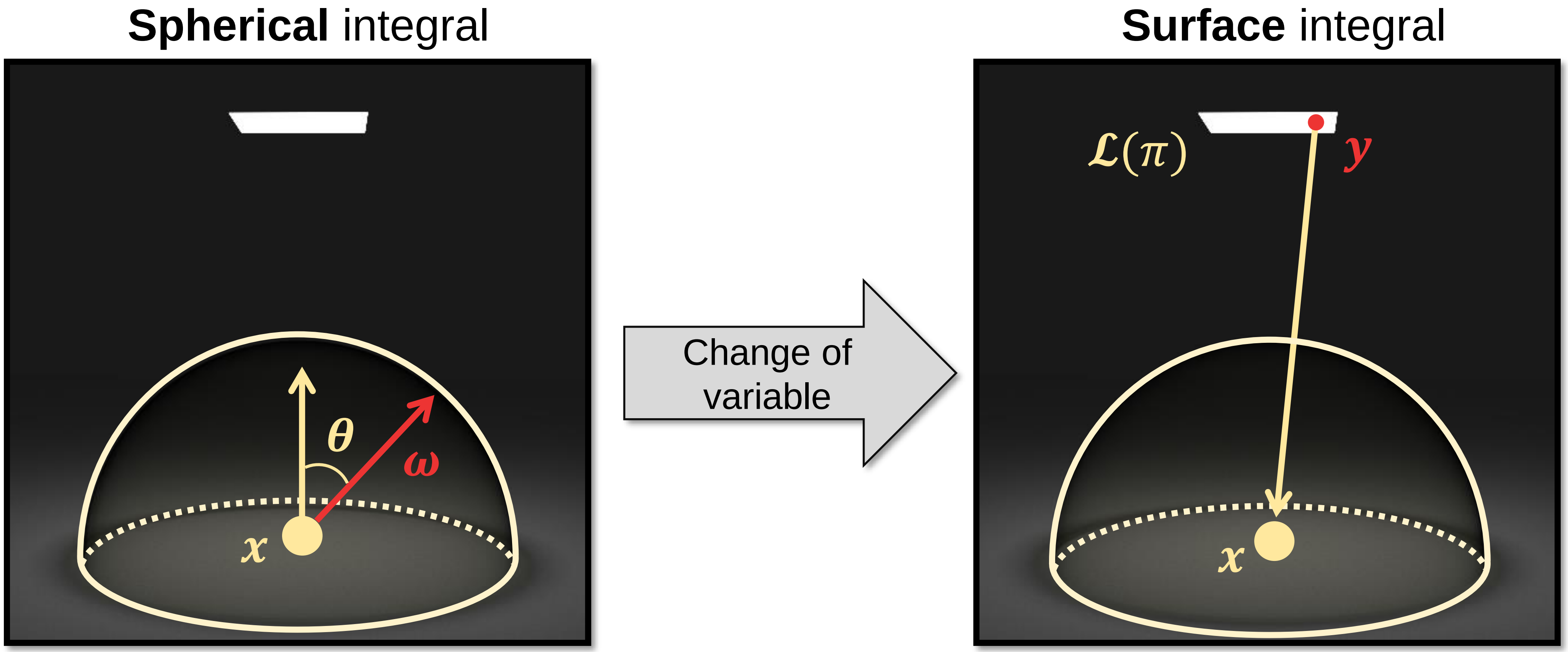

$$E = \int_{\mathbb{H}^2} L_i(\boldsymbol{\omega}) \cos\theta \, \mathrm{d}\sigma(\boldsymbol{\omega})$$

$$E = \int_{\mathcal{L}(\pi)} L_e(\boldsymbol{y} \to \boldsymbol{x}) \, G(\boldsymbol{x}, \boldsymbol{y}) \, \mathrm{d}A(\boldsymbol{y})$$

Spherical integral

Surface integral

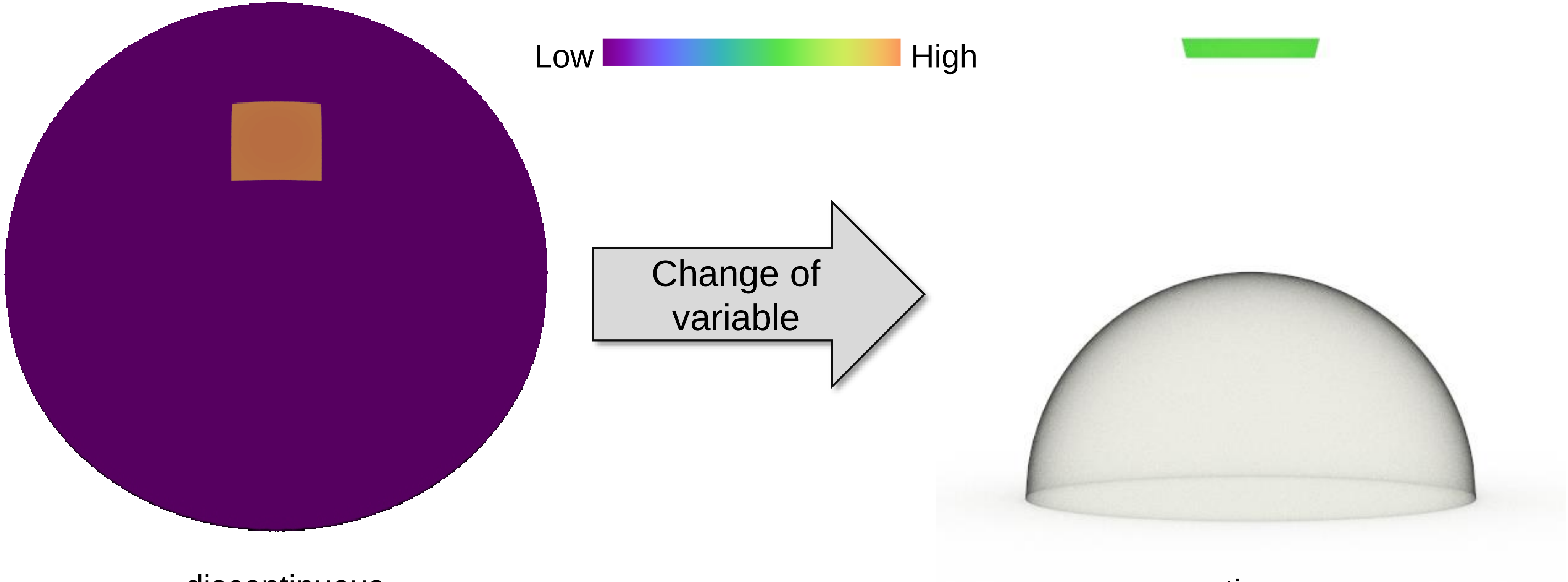

discontinuous

$$E = \int_{\mathbb{H}^2} L_i(\boldsymbol{\omega}) \cos\theta \, \mathrm{d}\sigma(\boldsymbol{\omega})$$

constant domain

continuous

$$E = \int_{\mathcal{L}(\pi)} L_e(\boldsymbol{y} \to \boldsymbol{x}) \, G(\boldsymbol{x}, \boldsymbol{y}) \, \mathrm{d}A(\boldsymbol{y})$$

evolving domain

DIFFERENTIAL IRRADIANCE

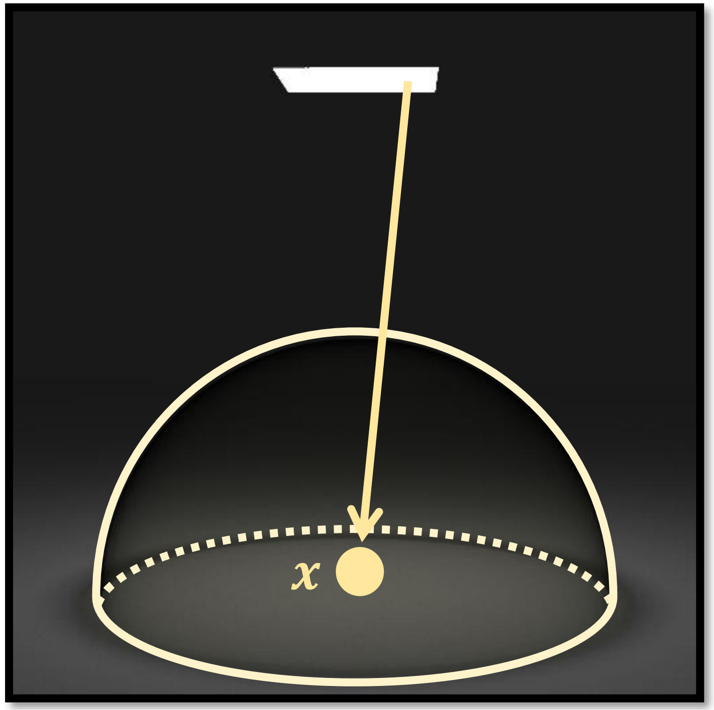

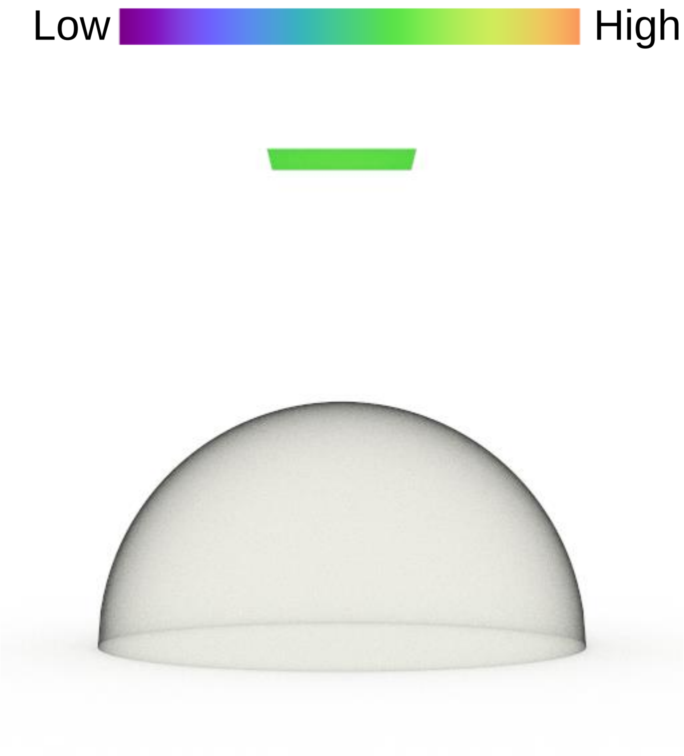

$$E = \int_{\mathcal{L}(\pi)} \overbrace{L_e(\boldsymbol{y} \to \boldsymbol{x}) G(\boldsymbol{x}, \boldsymbol{y})}^{f} \mathrm{d}A(\boldsymbol{y})$$

Differentiation →

A generalization of Reynolds theorem

$$\frac{\mathrm{d}E}{\mathrm{d}\pi} = \underbrace{\int_{\mathcal{L}(\pi)} \frac{\mathrm{d}f}{\mathrm{d}\pi} \mathrm{d}A}_{\text{Interior}} + \underbrace{\int_{\partial\mathcal{L}(\pi)} g \, \mathrm{d}l}_{\text{Boundary}}$$

Boundary $\neq 0$

REPARAMETERIZATION

$$E = \int_{\mathcal{L}(\pi)} L_e(\boldsymbol{y} \to \boldsymbol{x})\, G(\boldsymbol{x}, \boldsymbol{y})\, \mathrm{d}A(\boldsymbol{y})$$

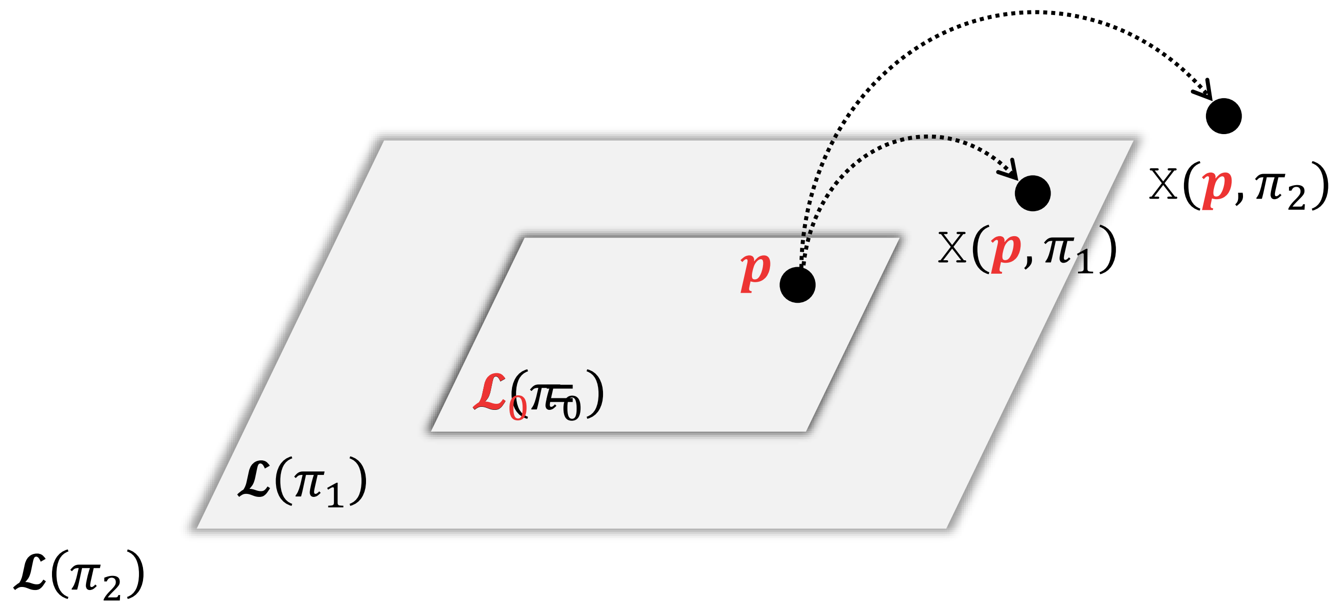

Parameterize $\mathcal{L}(\pi)$ using some fixed $\mathcal{L}_0$:

$$\boldsymbol{y} = \mathrm{X}(\boldsymbol{p}, \pi)$$

where $\mathrm{X}(\cdot\,, \pi)$ is one-to-one and continuous

Reparameterization with $\boldsymbol{y} = \mathrm{X}(\boldsymbol{p}, \pi)$:

$$E = \int_{\mathcal{L}_0} L_e(\boldsymbol{y} \to \boldsymbol{x}) G(\boldsymbol{x}, \boldsymbol{y}) \left| \frac{\mathrm{d}A(\boldsymbol{y})}{\mathrm{d}A(\boldsymbol{p})} \right| \mathrm{d}A(\boldsymbol{p})$$

REPARAMETERIZATION

$$E = \int_{\mathcal{L}(\pi)} \overbrace{L_e(\boldsymbol{y} \to \boldsymbol{x})\, G(\boldsymbol{x}, \boldsymbol{y})}^{f}\, \mathrm{d}A(\boldsymbol{y})$$

$$\frac{\mathrm{d}E}{\mathrm{d}\pi} = \underbrace{\int_{\mathcal{L}(\pi)} \frac{\mathrm{d}f}{\mathrm{d}\pi}\, \mathrm{d}A}_{=\,0} + \underbrace{\int_{\partial\mathcal{L}(\pi)} g\, \mathrm{d}l}_{\neq\,0}$$

$$\boldsymbol{y} = \mathrm{X}(\boldsymbol{p}, \pi)$$

$$E = \int_{\mathcal{L}_0} \overbrace{L_e(\boldsymbol{y} \to \boldsymbol{x})\, G(\boldsymbol{x}, \boldsymbol{y}) \left| \frac{\mathrm{d}A(\boldsymbol{y})}{\mathrm{d}A(\boldsymbol{p})} \right|}^{f_0} \mathrm{d}A(\boldsymbol{p})$$

$$\frac{\mathrm{d}E}{\mathrm{d}\pi} = \underbrace{\int_{\mathcal{L}_0} \frac{\mathrm{d}f_0}{\mathrm{d}\pi}\, \mathrm{d}A}_{\neq\,0} + \underbrace{\int_{\partial\mathcal{L}_0} g_0\, \mathrm{d}l}_{=\,0}$$

REPARAMETERIZATION

Reparameterization for irradiance

$$E = \int_{\mathcal{L}(\pi)} L_e(\boldsymbol{y} \to \boldsymbol{x}) G(\boldsymbol{x}, \boldsymbol{y}) \mathrm{d}A(\boldsymbol{y})$$

$\boldsymbol{y} = \mathrm{X}(\boldsymbol{p}, \pi)$

$$E = \int_{\mathcal{L}_0} L_e(\boldsymbol{y} \to \boldsymbol{x})\, G(\boldsymbol{x}, \boldsymbol{y}) \left| \frac{\mathrm{d}A(\boldsymbol{y})}{\mathrm{d}A(\boldsymbol{p})} \right| \mathrm{d}A(\boldsymbol{p})$$

↑ Fixed surface

Reparameterization for path integral

$$I = \int_{\Omega(\pi)} f(\bar{\boldsymbol{x}})\, \mathrm{d}\mu(\bar{\boldsymbol{x}})$$

$\bar{\boldsymbol{x}} = \mathrm{X}(\bar{\boldsymbol{p}}, \pi)$

$$I = \int_{\Omega_0} f(\bar{\boldsymbol{x}}) \left| \frac{\mathrm{d}\mu(\bar{\boldsymbol{x}})}{\mathrm{d}\mu(\bar{\boldsymbol{p}})} \right| \mathrm{d}\mu(\bar{\boldsymbol{p}})$$

Fixed path space ↑

$$\left| \frac{\mathrm{d}\mu(\bar{\boldsymbol{x}})}{\mathrm{d}\mu(\bar{\boldsymbol{p}})} \right| = \prod_i \left| \frac{\mathrm{d}A(\boldsymbol{x}_i)}{\mathrm{d}A(\boldsymbol{p}_i)} \right|$$

DIFFERENTIAL PATH INTEGRAL

Original

$$I = \int_{\Omega(\pi)} f(\bar{\boldsymbol{x}})\, \mathrm{d}\mu(\bar{\boldsymbol{x}})$$

$$\bar{\boldsymbol{x}} = \mathrm{X}(\bar{\boldsymbol{p}}, \pi)$$

Reparameterized

$$I = \int_{\Omega_0} f(\bar{\boldsymbol{x}}) \left| \frac{\mathrm{d}\mu(\bar{\boldsymbol{x}})}{\mathrm{d}\mu(\bar{\boldsymbol{p}})} \right| \mathrm{d}\mu(\bar{\boldsymbol{p}})$$

Original

$$\frac{\mathrm{d}I}{\mathrm{d}\pi} = \int_{\Omega(\pi)} \frac{\mathrm{d}f(\bar{\boldsymbol{x}})}{\mathrm{d}\pi}\, \mathrm{d}\mu(\bar{\boldsymbol{x}}) + \int_{\partial\Omega(\pi)} g(\bar{\boldsymbol{x}}) \mathrm{d}\mu'(\bar{\boldsymbol{x}})$$

Pro: No global parametrization required

Con: More types of discontinuities

Reparameterized

$$\frac{\mathrm{d}I}{\mathrm{d}\pi} = \int_{\Omega_0} \frac{\mathrm{d}}{\mathrm{d}\pi} \left(f(\bar{\boldsymbol{x}}) \left| \frac{\mathrm{d}\mu(\bar{\boldsymbol{x}})}{\mathrm{d}\mu(\bar{\boldsymbol{p}})} \right| \right) \mathrm{d}\mu(\bar{\boldsymbol{p}}) + \int_{\partial\Omega_0} g(\bar{\boldsymbol{p}}) \mathrm{d}\mu'(\bar{\boldsymbol{p}})$$

Pro: Fewer types of discontinuities

Con: Requires global parametrization X

DIFFERENTIAL PATH INTEGRAL

Differential path integral

$$\frac{\mathrm{d}I}{\mathrm{d}\pi} = \int_{\Omega(\pi)} \frac{\mathrm{d}f(\bar{x})}{\mathrm{d}\pi}\,\mathrm{d}\mu(\bar{x}) + \int_{\partial\Omega(\pi)} g(\bar{x})\,\mathrm{d}\mu'(\bar{x})$$

$$\frac{\mathrm{d}I}{\mathrm{d}\pi} = \int_{\Omega_0} \frac{\mathrm{d}}{\mathrm{d}\pi}\left(f(\bar{x})\left|\frac{\mathrm{d}\mu(\bar{x})}{\mathrm{d}\mu(\bar{p})}\right|\right)\mathrm{d}\mu(\bar{p}) + \int_{\partial\Omega_0} g(\bar{p})\,\mathrm{d}\mu'(\bar{p})$$

Topology-driven

Visibility-driven

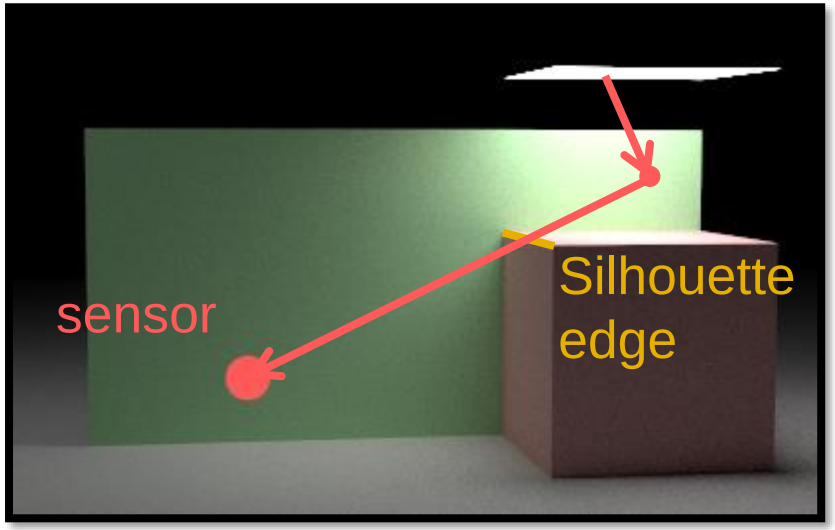

MONTE CARLO ESTIMATORS

ESTIMATING INTERIOR INTEGRAL

(Reparameterized)
Differential path Integral

$$\frac{\partial I}{\partial \pi} = \int_{\Omega_0} \frac{\partial}{\partial \pi}\left(f(\overline{\boldsymbol{x}}) \left| \frac{\mathrm{d}\mu(\overline{\boldsymbol{x}})}{\mathrm{d}\mu(\overline{\boldsymbol{p}})} \right| \right) \mathrm{d}\mu(\overline{\boldsymbol{p}}) + \int_{\partial\Omega_0} g(\overline{\boldsymbol{p}}) \mathrm{d}\mu'(\overline{\boldsymbol{p}})$$

Interior integral

Boundary integral

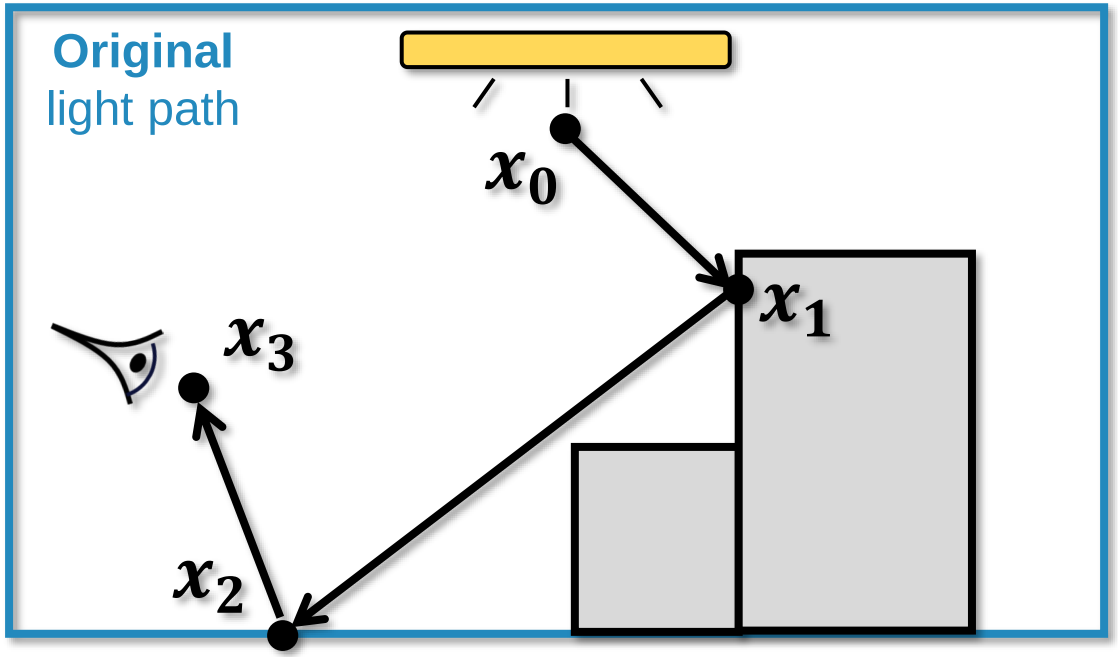

- Can be estimated using identical path sampling strategies as forward rendering
  - Unidirectional path tracing
  - Bidirectional path tracing
  - …

Different MC estimators

(Reparameterized)
Differential path Integral

$$\frac{\partial I}{\partial \pi} = \int_{\Omega_0} \frac{\partial}{\partial \pi}\left(f(\bar{\boldsymbol{x}}) \left| \frac{\mathrm{d}\mu(\bar{\boldsymbol{x}})}{\mathrm{d}\mu(\bar{\boldsymbol{p}})} \right| \right) \mathrm{d}\mu(\bar{\boldsymbol{p}}) + \int_{\partial\Omega_0} g(\bar{\boldsymbol{p}}) \mathrm{d}\mu'(\bar{\boldsymbol{p}})$$

Boundary integral

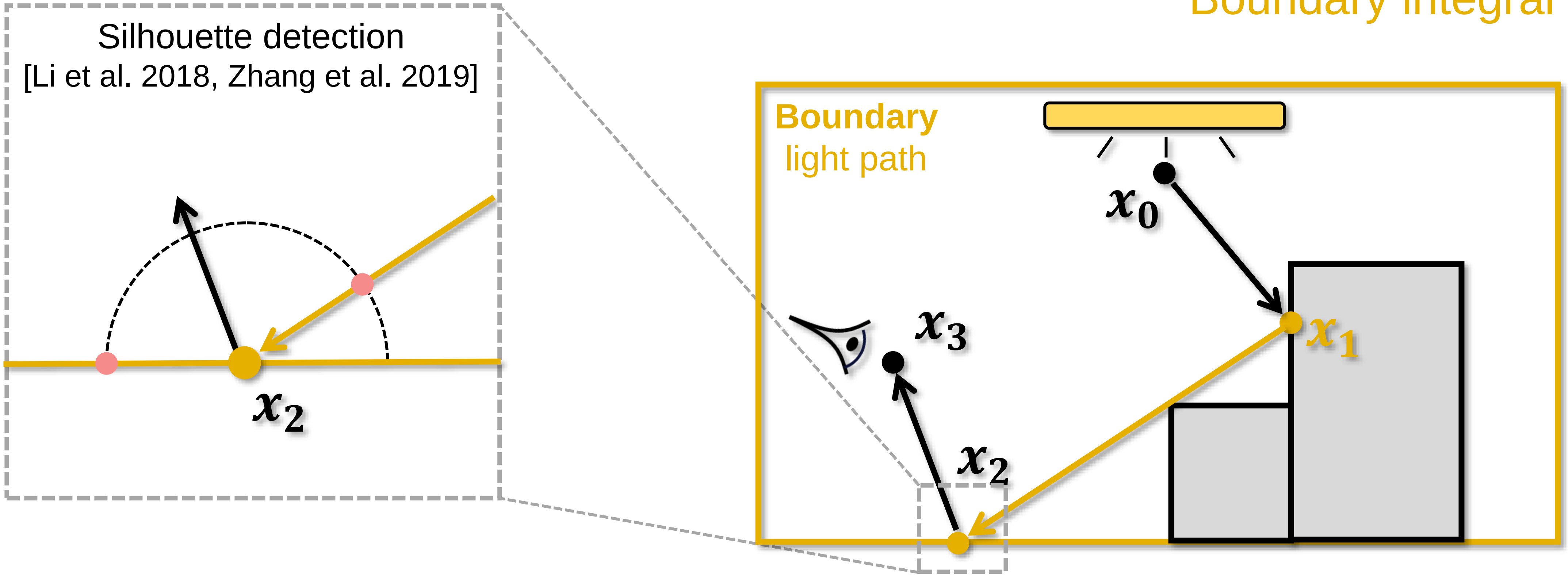

ESTIMATING BOUNDARY INTEGRAL

(Reparameterized)
Differential path Integral

$$\frac{\partial I}{\partial \pi} = \int_{\Omega_0} \frac{\partial}{\partial \pi}\left(f(\overline{\boldsymbol{x}}) \left|\frac{\mathrm{d}\mu(\overline{\boldsymbol{x}})}{\mathrm{d}\mu(\overline{\boldsymbol{p}})}\right|\right) \mathrm{d}\mu(\overline{\boldsymbol{p}}) + \int_{\partial\Omega_0} g(\overline{\boldsymbol{p}}) \mathrm{d}\mu'(\overline{\boldsymbol{p}})$$

where $\overline{\boldsymbol{x}} = \mathrm{X}(\overline{\boldsymbol{p}}, \pi)$

Boundary integral

- Construct boundary segment
- Construct source and sensor subpaths
- To improve efficiency
  - Next-event estimation
  - Importance sampling of boundary segments

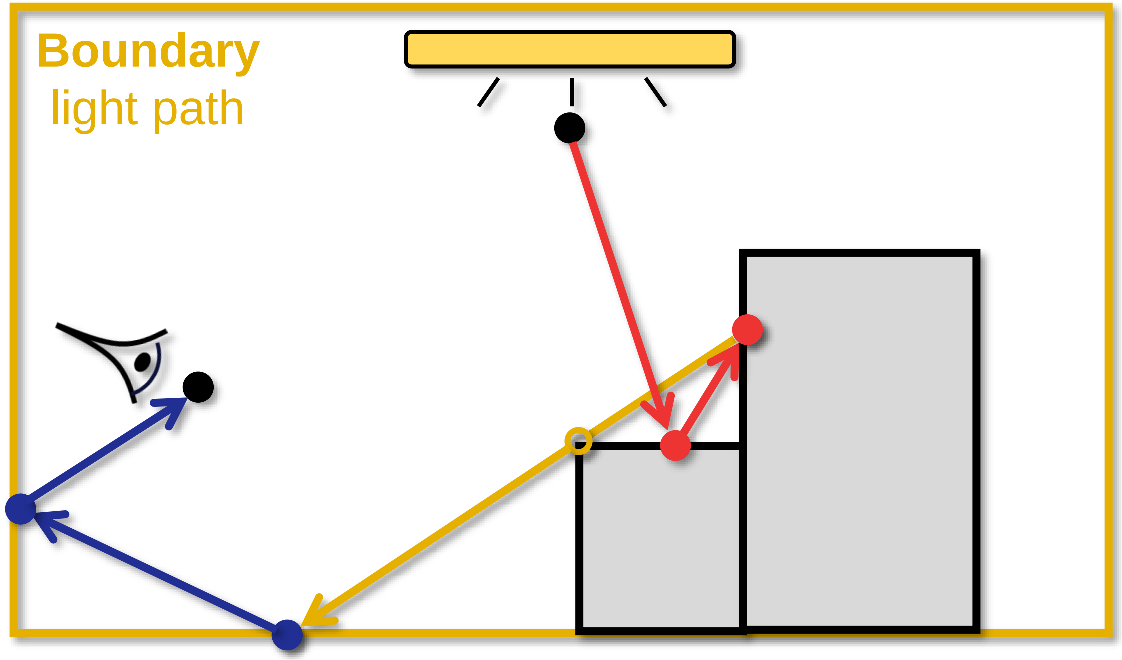

OUR ESTIMATORS

Unidirectional estimator

Interior: **unidirectional** path tracing

Boundary: **unidirectional** sampling of subpaths

Bidirectional estimator

Interior: **bidirectional** path tracing

Boundary: **bidirectional** sampling of subpaths

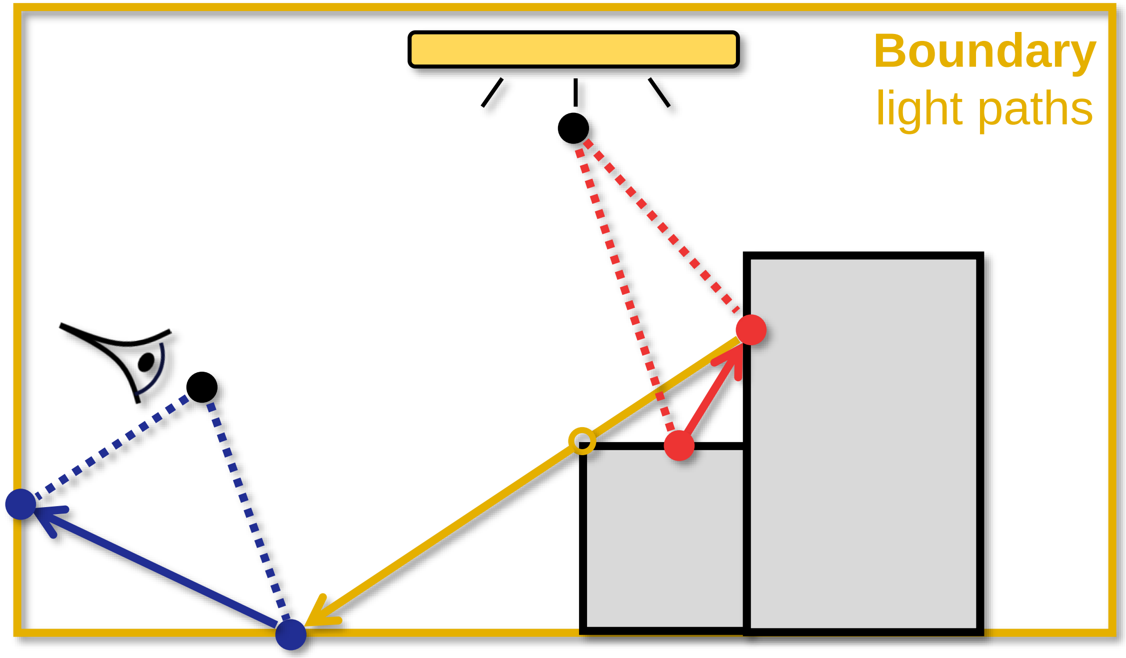

Unidirectional path tracing + NEE

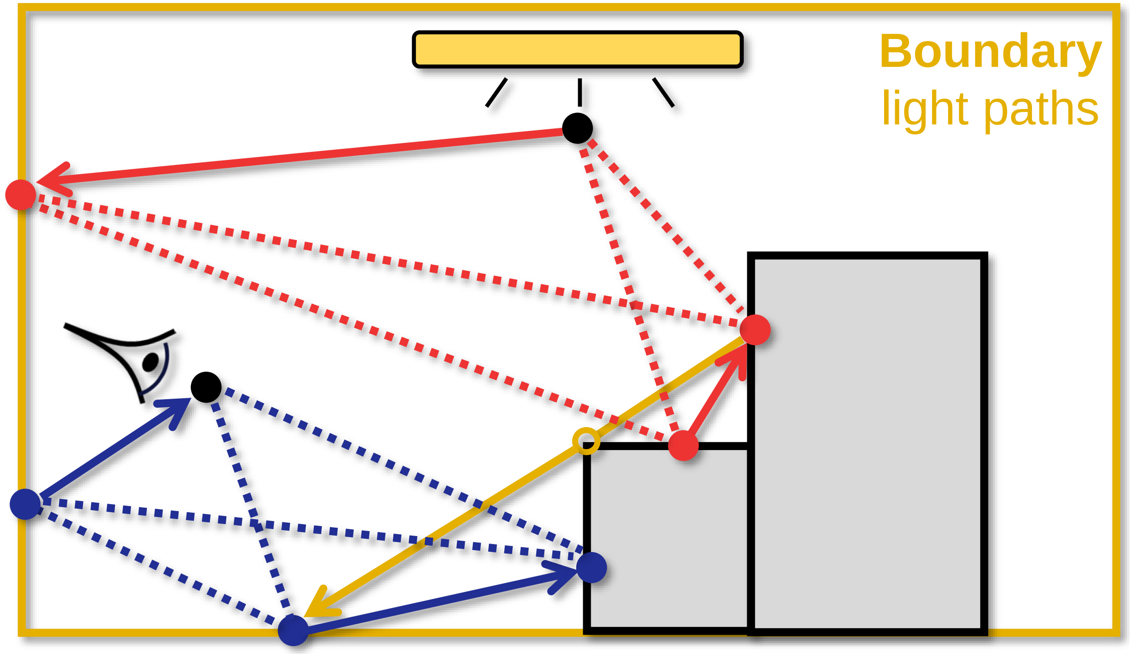

Bidirectional path tracing

RESULTS

RESULTS

COMPLEX GEOMETRY

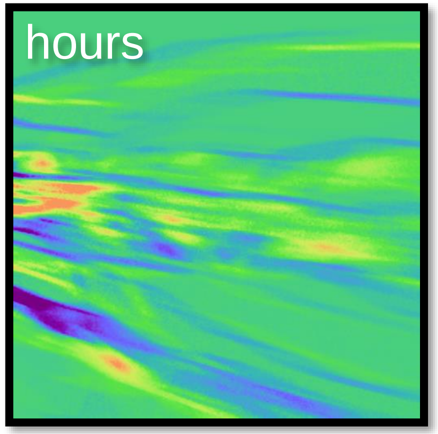

Reference

Equal-sample comparison

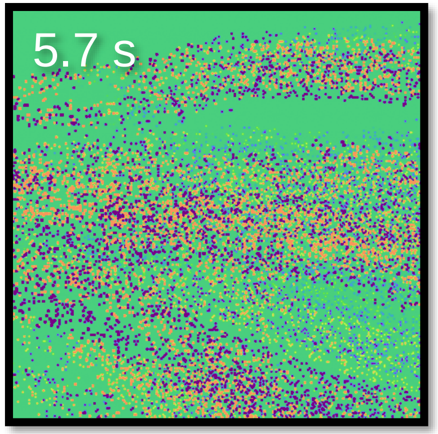

[Zhang et al. 2019]

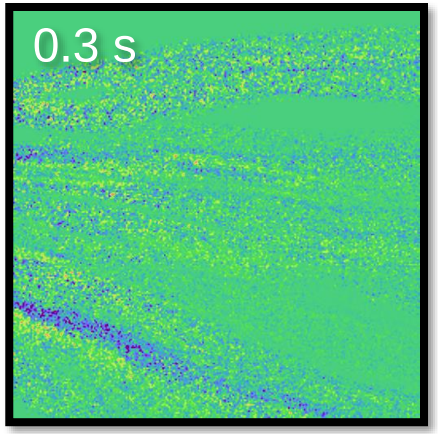

[Loubet et al. 2019]

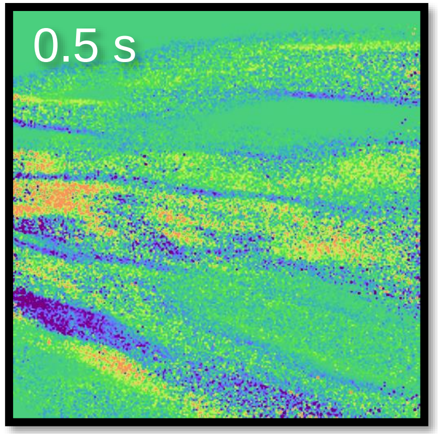

Ours

RESULTS
COMPLEX GEOMETRY

Target image

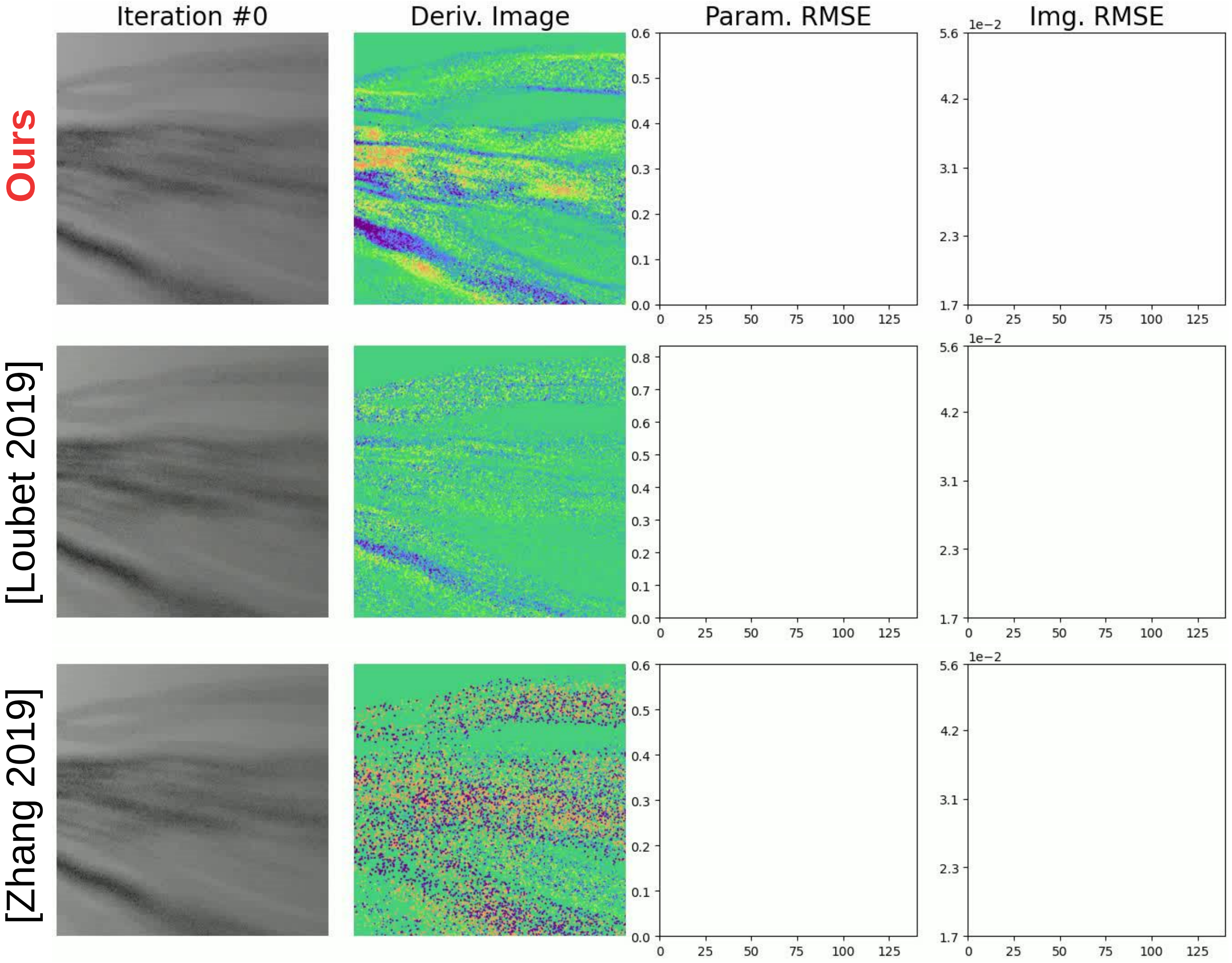

- Optimizing *rotation angle*
- **Equal-sample** per iteration
- **Identical** optimization setting
  - Learning rate (Adam)
  - Initializations

RESULTS

COMPLEX LIGHT TRANSPORT EFFECTS

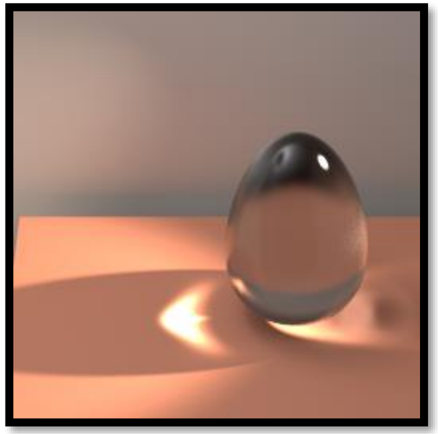

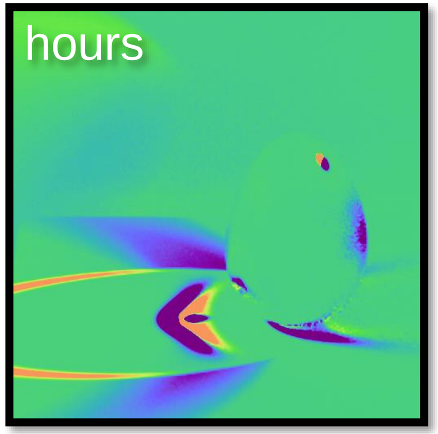

Reference

Equal-sample comparison

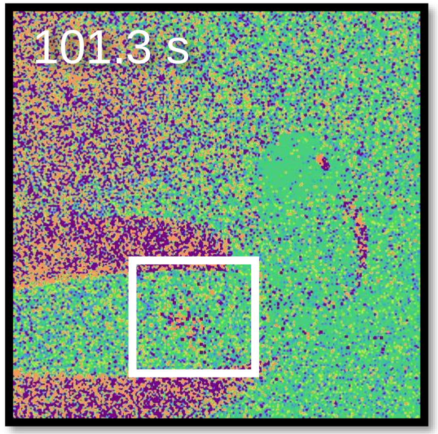

[Zhang et al. 2019]

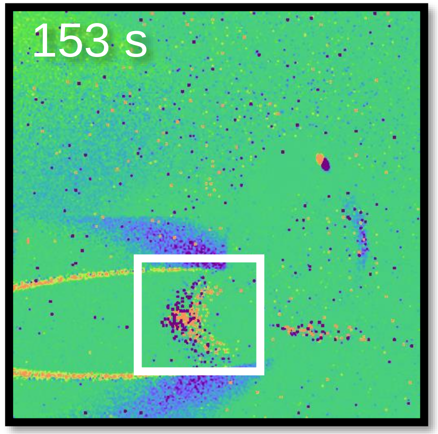

[Loubet et al. 2019]

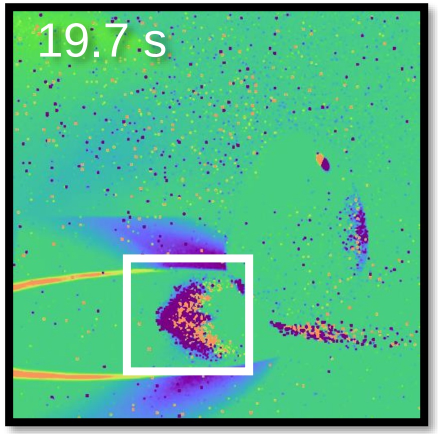

Ours (unidirectional)

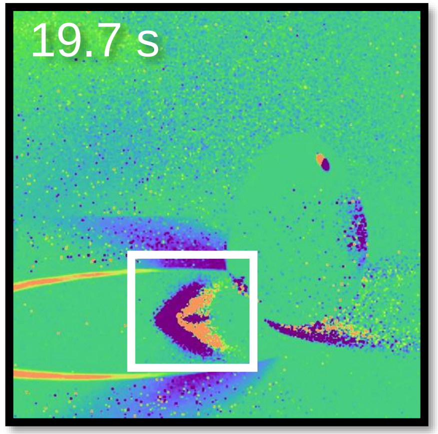

Ours (bidirectional)

RESULTS

COMPLEX LIGHT TRANSPORT EFFECTS

Target image

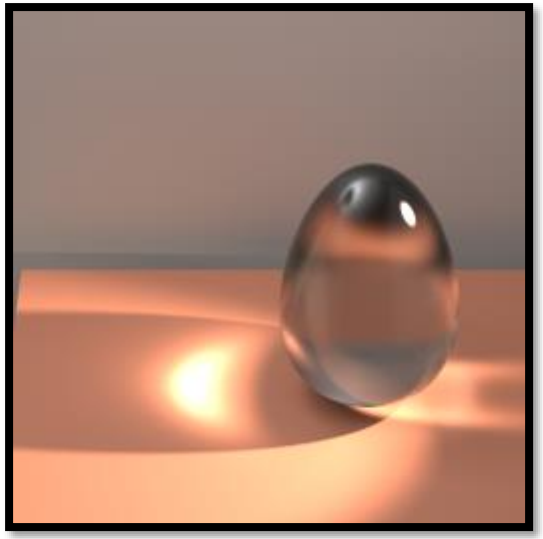

- Optimizing
  - Glass IOR
  - Spotlight position
- **Equal-time** per iteration
- **Identical** optimization setting

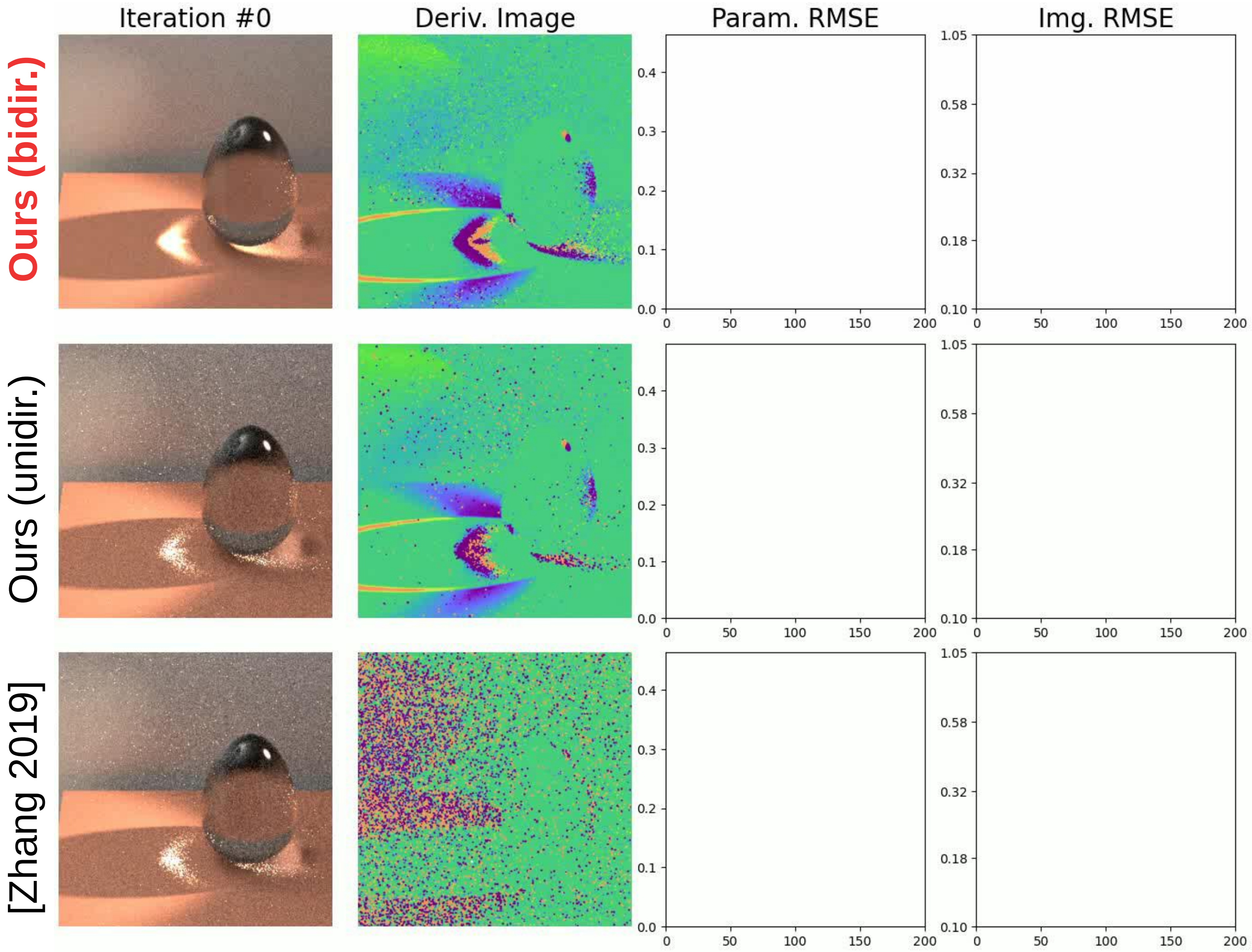

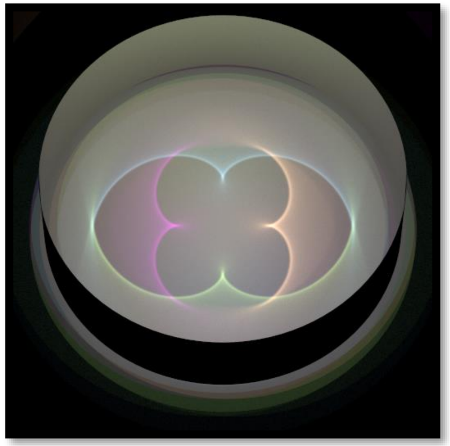

Initial

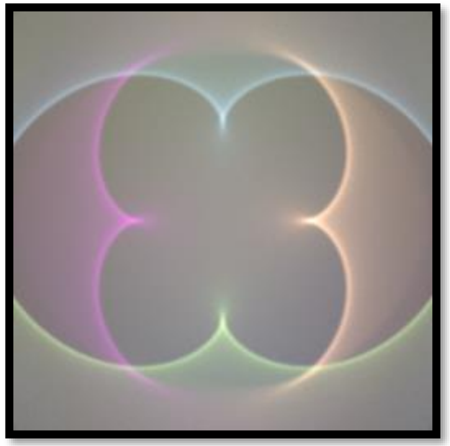

Optimizing **cross-sectional** shape (100 variables)

Target image

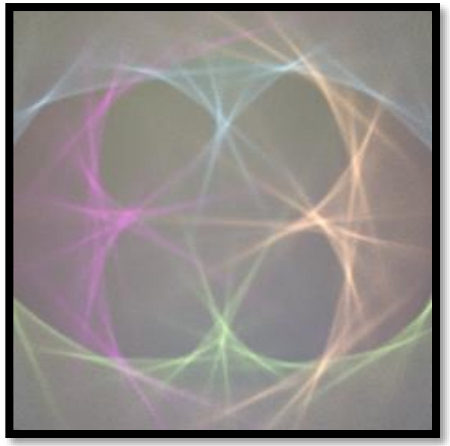

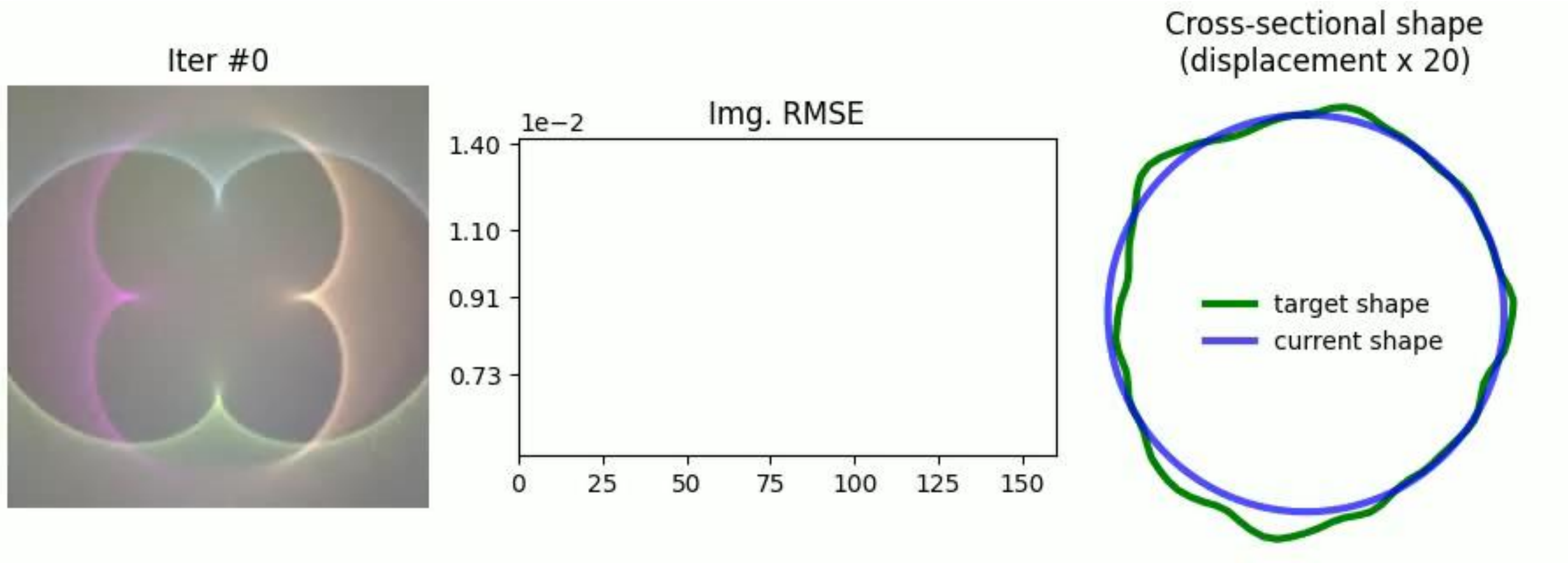

RESULTS

Original image

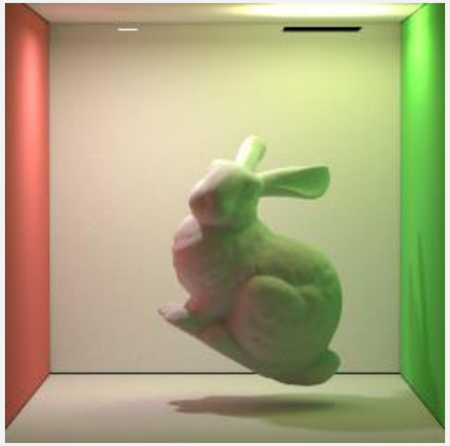

Derivative image

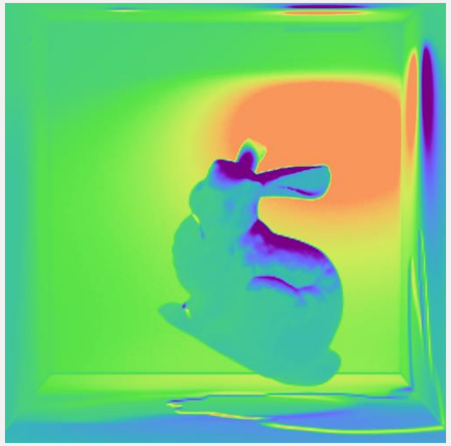

Original image

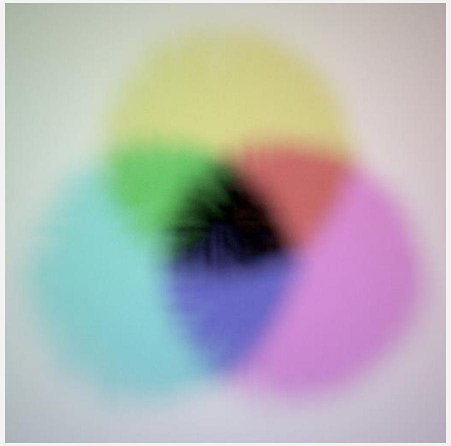

Derivative image

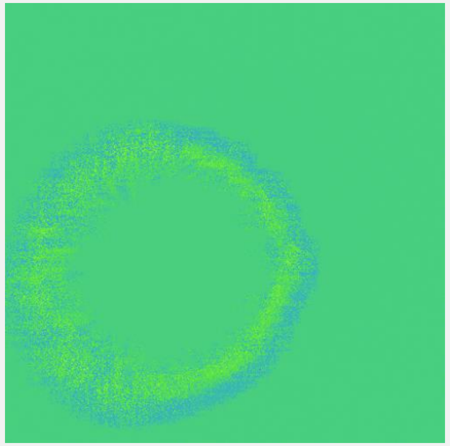

Config.

Optimize (initial)

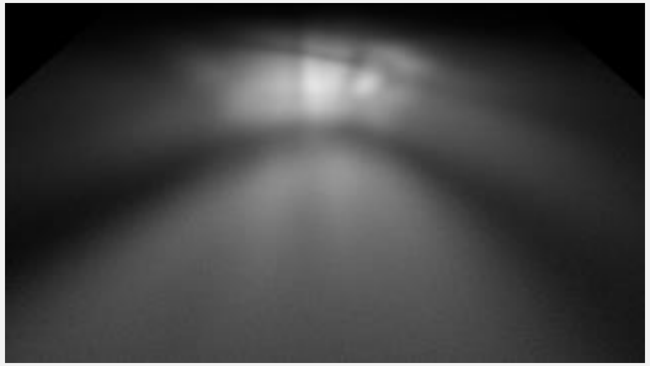

Optimize (final)

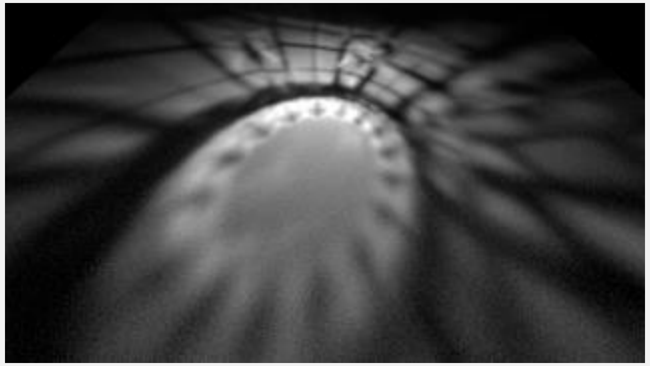

Target

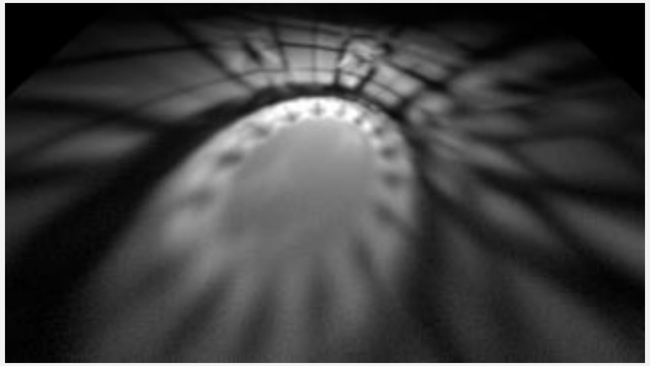

LIMITATIONS AND FUTURE WORK

- Surface-based light transport
- More sophisticated Monte Carlo estimators
  - *Markov-chain Monte Carlo* (MCMC) methods
- Better importance sampling of paths

CONCLUSION

- Differential path integral
  - Separated *interior* and *boundary*

$$\int_{\Omega} \frac{\mathrm{d}}{\mathrm{d}\pi} f(\overline{\boldsymbol{x}})\mathrm{d}\mu(\overline{\boldsymbol{x}}) + \int_{\partial\Omega} g(\overline{\boldsymbol{x}})\mathrm{d}\mu'(\overline{\boldsymbol{x}})$$

Interior integral — Boundary integral

- Reparameterization
  - Only need to consider silhouette edges

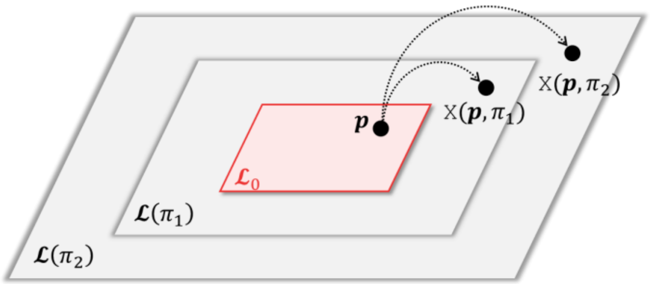

- Unbiased Monte Carlo methods
  - Unidirectional and bidirectional estimators
  - No silhouette detection is needed

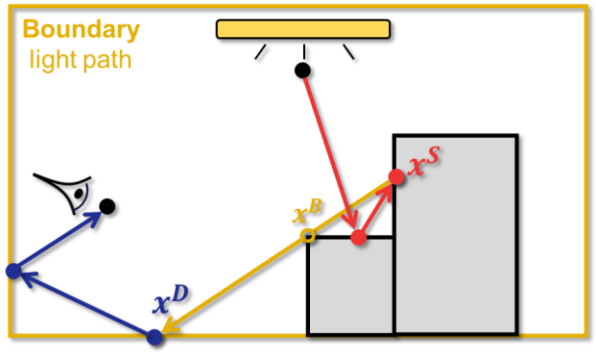

ACKNOWLEDGMENTS

- Anonymous reviewers
- Funding
  - NSF grants 1730147, 1900849 and 1900927
  - AWS Cloud Credits for Research program

Project webpage

https://rb.gy/lb2z3s

Thank you!